


STRUCTURE AND FORMATION OF THE PERFORATED THECA DEFINING THE PELAGOPHYCEAE (HETEROKONTA), AND THREE NEW GENERA THAT SUBSTANTIATE THE DIVERSE NATURE OF THE CLASS¹

Richard Wetherbee,² Trevor T. Bringloe , Allison van de Meene

School of BioSciences, University of Melbourne, Melbourne, Victoria, 3010, Australia

Robert A. Andersen

Friday Harbor Laboratories, University of Washington, Seattle, Washington, USA

and Heroen Verbruggen ²

School of BioSciences, University of Melbourne, Melbourne, Victoria, 3010, Australia

The pelagophytes, a morphologically diverse class of marine heterokont algae, have been historically united only by DNA sequences. Recently we described a novel perforated theca (PT) encasing cells from the Pelagophyceae and hypothesized it may be the first morphological feature to define the class. Here we consolidate that observation, describing a PT for the first time in an additional seven pelagophyte genera, including three genera new to science. We established clonal cultures of pelagophytes collected from intertidal pools located around Australia, and established phylogenetic trees based on nuclear 18S rDNA and plastid *rbcL*, *psaA*, *psaB*, *psbA* and *psbC* gene sequences that led to the discovery of three new species: *Wyeophycus julieharrissiae* and *Chromopallida australis* form a distinct lineage along with *Ankylochrysis lutea* within the Pelagomonadales, while *Pituiglomerulus capricornicus* is sister genus to *Chrysocystis fragilis* in the Chrysocystaceae (Sarcinochrysidales). Using fixation by high-pressure freezing for electron microscope observations, a distinctive PT was observed in the three new genera described in this paper, as well as four genera not previously investigated: *Chrysoreinhardia*, *Sargassococcus*, *Sungminbooa* and *Andersenina*. The mechanism of PT formation is novel, being fabricated from rafts in Golgi-derived vesicles before being inserted into an established PT. Extracellular wall and/or mucilage layers assemble exterior to the PT in most pelagophytes, the materials likewise secreted by Golgi-derived vesicles, though the mechanism of secretion is novel. Secretory vesicles never fuse with the plasma membrane as in classic secretion and deposition, but rather relocate extracellularly

beneath the PT and disintegrate, the contents having to pass through the PT prior to wall and/or mucilage synthesis. This study substantiates the diverse nature of pelagophytes, and provides further evidence that the PT is a sound morphological feature to define the Pelagophyceae, with all 14 of the 20 known genera studied to date by TEM possessing a PT.

Key index words: *Chromopallida*; Chrysocystaceae; Golgi vesicle secretion; molecular phylogeny; Pelagomonadales; Pelagophyceae; perforated theca; *Pituiglomerulus*; Sand-dwelling; Sarcinochrysidaceae; *Wyeophycus*

ABBREVIATIONS: HPF, high-pressure freezing; ML, maximum likelihood; OTU, operational taxonomic unit; PM, plasma membrane; PT, perforated theca

The class Pelagophyceae was formed when DNA sequences revealed a highly unusual, truly unflagellate organism not related to other heterokont classes (Andersen et al. 1993). Additional studies using molecular markers confirmed that, in addition to the order Pelagomonadales, the order Sarcinochrysidales (Gayral and Billard 1977) belonged in the Pelagophyceae (Saunders et al. 1997, Han et al. 2018). The Pelagophyceae is morphologically diverse and all described species are exclusively marine. Furthermore, most species are found along coastlines, with *Pelagomonas* and *Pelagococcus* being the only true open ocean taxa. Currently, the Pelagophyceae contains 17 known genera and all species are described with DNA sequences. Additional taxa may well be included in the pelagophytes once several suspect species have been isolated and DNA sequences obtained (for example, see Han et al. 2018). With regard to harmful algal blooms, *Aureococcus anophagefferens* impacts shellfish

¹Received 18 July 2022. Accepted 10 October 2022.

²Authors for correspondence: e-mail richardw@unimelb.edu.au; heroen@unimelb.edu.au.

Editorial Responsibility: J.M. Cock (Associate Editor)

production (Bricelj and Lonsdale 1997, Gobler et al. 2011), and *Aureoumbra lagunensis* produced the world's longest algal bloom of over eight continuous years (Buskey et al. 2001).

When first described, the phylogenetic position of the Pelagophyceae was unresolved, although it was speculated that the Pelagophyceae might be related to the Dictyochophyceae, Pedinellophyceae (now included in the Dictyophyceae) and diatoms (Andersen et al. 1993). Shortly thereafter, the Pelagophyceae were shown to be sister to the Dictyochophyceae in a cladistic analysis of morphological and biochemical features, and these two classes were, in turn, sister to the diatoms (Saunders et al. 1995). This study suggested a clade (diatoms, dictyochophytes, pelagophytes) consisting of highly reduced flagellar apparatuses for the swimming cells. However, when the Sarcinochrysidales was added to the Pelagophyceae (Saunders et al. 1997), the morphological argument was weakened because of the well-developed flagellar system of the Sarcinochrysidales. Nevertheless, all recent molecular studies consistently placed the Pelagophyceae sister to the Dictyochophyceae, with the diatoms and bolidophytes sister to the Pelagophyceae/Dictyochophyceae (Yang et al. 2012, Derelle et al. 2016, Dorrell and Bowler 2016, Dorrell et al. 2017, Han et al. 2018, Wetherbee et al. 2019b).

All pelagophyte genera that have been studied with TEM were observed to possess a single, recently proposed morphological feature to unite the class, a novel cell covering termed a perforated theca (PT; Wetherbee et al. 2021). The PT is a dense outer covering or sheath penetrated by distinctive pores that encloses benthic cells as well as flagellates and zoospores except where flagella emerge. At least two layers define the PT, a largely transparent, fibrous layer sandwiched between the plasma membrane and an outer electron dense, perforated layer. Multilayered PTs were also observed in species eventually assigned to the Pelagophyceae by gene sequencing, and though pores were not mentioned, they were observed in published micrographs (see references below).

Pelagophyte species range in size from a $1.5 \times 2\text{--}3 \mu\text{m}$ flagellate (*Pelagomonas*; Andersen et al. 1993), to macroscopic sheets 1 cm across (*Aureoscheda*; Wynne et al. 2014) and flowing colonies 3–5 cm long (*Chrysocystis*; Lobban et al. 1995, Wynne et al. 2014). The planktonic forms are flagellate (*Pelagomonas*, *Ankylochrysis*; Andersen et al. 1993, Honda and Inouye 1995) or coccoid (*Aureococcus*, *Aureoumbra*, *Pelagococcus*; Lewin et al. 1977, Sieburth et al. 1988, DeYoe et al. 1997), whereas the attached species are predominantly capsoid organisms with vegetative cell division (*Arachnocyrtis*, *Chrysocystis*, *Chrysosphaeum*, *Chrysoreinhardia*, *Glomerochrysis*, *Pelagospilus*, *Sarcinochrysis*, *Sargassococcus*, *Sungminbooa* and an Australian species of *Aureoumbra*; Han et al. 2018, Davison and Bewley 2019, Wetherbee et al. 2021).

One genus has both a benthic unicellular species and a large colonial species (*Gazia*; Wetherbee et al. 2021), and one genus with a filamentous form is known (*Andersenella*; Wetherbee et al. 2015). Heterokont zoospores are produced by many genera, possessing an anterior flagellum bearing mastigonemes that beats as a sinusoidal wave and a short, stiff posterior flagellum that beats with a sculling motion.

During our exploration of sand-dwelling microalgae collected around Australia (Grant et al. 2011, 2013, Wetherbee et al. 2015, 2019a, b, 2021, Wetherbee and Verbruggen 2016, Graf et al. 2020), we discovered several unknown pelagophytes. The goal of this study was to describe three new pelagophyte taxa, the sand-dwelling species *Wyeophycus julieharrissiae* and *Pituiglomerulus capricornicus* in addition to the planktonic flagellate *Chromopallida australis*, and to infer their phylogenetic position among the pelagophytes. Our approach consisted of light and electron-microscopic observations of culture strains, and phylogenetic inference based from multimarker datasets.

In addition to the three new genera described here, another major goal was to further document the presence of a PT in previously unexamined genera from the Pelagophyceae: *Chrysoreinhardia*, *Sargassococcus*, *Sungminbooa* and *Andersenella*. At present 14 of the known 20 pelagophyte genera, including the three new genera described here, have been found by our investigations, or observed in published papers by other researchers, to possess a PT. We, therefore, confirm our hypothesis that the PT is present in all the major lineages of the class, the first morphological feature shown to characterize the pelagophytes. In addition to extending our knowledge of the structure and distribution of the PT in the class, our second goal was to determine the role of the endomembrane system in PT formation and secretion, as well as the secretion of materials destined for the production of the extracellular matrix (ECM; cell walls and/or mucilage layers) external to the PT, a feature of many pelagophyte species.

MATERIALS AND METHODS

Sampling, isolation, and culture. New sequences of all species listed below were submitted to GenBank (see Table S1 and Fig. S1 in the Supporting Information). The sample containing *Wyeophycus julieharrissiae* was collected in a shallow pool south of the Wye River beach, Great Ocean Road, Wye River, Victoria ($38^{\circ}38'20''$ S; $143^{\circ}53'34''$ E), in April 2016 by R. Wetherbee (CSIRO strain CS-1474). The sample consisted of approximately $0.5\text{--}1.0 \text{ cm}^3$ of sand plus seawater that was placed into a 60 mL culture flask and returned to the lab. A clonal culture (Wye36) was established by isolating flagellates from the field sample by micro-pipetting into K-enriched seawater medium (Keller et al. 1987). The culture was maintained in 60 mL plastic containers at 21°C under Sylvania 58 Luxline Plus and Gro-Lux fluorescent lamps with a daily 10:14 h light:dark cycle; a stock culture was transferred into new K-medium once a month. A sand/water sample

containing *Chromopallida australis* was collected in an intertidal pool, Trial Bay, Tasmania, Australia (43°07054' S; 147°15019' E) in April 2009 by B. Grant, and a clonal culture established as described above (CSIRO strain CS-1472). A sand sample containing *Pituiglomerulus capricornicus* was collected from a large intertidal pool at Heron Island, Queensland (23°26'38.9" S; 151°54'53.5" E) in February, 2020 by M. Pasella and a clonal culture was established as described above (CSIRO strain CS-1473).

We also isolated clonal cultures of a strain of *Chrysoeinhardia giraudii* from a intertidal lagoon at Heron Island, Queensland (23°26'38.9" S; 151°54'53.5" E) in February, 2020 by M. Pasella (CSIRO strain CS-1476), *Sargassococcus* sp. from an intertidal pool at Wye River, Victoria (38°38'20" S; 143°53'34" E) in April, 2018 by R. Wetherbee (CSIRO strain CS-1477) and *Sungminbooa* sp. from an high intertidal pool, Narooma Inlet, New South Wales (36°207732 S; 150°125127 E) in March, 2015 by R. Wetherbee (CSIRO strain CS-1478) and maintained as described above. We also worked on a clonal culture of *Andersenina nodulosa* from an intertidal pool at Penguin beach, Tasmania (418060' S, 1468040' E) in February 2011 by B. Grant (CSIRO strain CS-1113) as described in Wetherbee et al. (2015). The identity of the *Chrysoeinhardia* and *Sargassococcus* strains were verified with 18 S sequences and the *Andersenina* strain is the type strain of the species.

Light microscopy. To observe the flagellate stage of *Wyeophycus julieharrissiae* and *Chromopallida australis*, a drop of cell culture was taken at the beginning of the light period when flagellates were most prevalent and mounted onto microscope slides with coverslips sealed with a 1:1:1 ratio of Vaseline, lanoline, and paraffin wax. For benthic cells of *W. julieharrissiae* and *Pituiglomerulus capricornicus*, 5 mL of culture containing flagellates and benthic cells was poured over coverslips in small petri dishes and allowed to settle and grow for 3–14 days. Coverslips were then removed and inverted onto microscope slides and mounted as above. Flagellates and benthic cells were observed and recorded using a Zeiss AxioPlan 2 microscope (Carl Zeiss, Oberkochen, Germany) and photographs were taken using a Canon EOS 60D digital single-lens reflex camera (Canon USA, Melville, NY, USA).

Transmission electron microscopy. Cells were prepared by high-pressure freezing (HPF; Wetherbee et al. 2019b). Benthic cells and/or flagellates of the three species studied were gently centrifuged and placed directly in Type A carriers without cryoprotectants and covered with the flat surface of the type B carrier before HPF using a Leica EM ICE high-pressure freezer (Leica Microsystems, Austria; see Wetherbee et al. 2019b). The cells were freeze substituted in 2% osmium tetroxide and 8% 2,2-Dimethoxypropane (DMP) in acetone for 72 h at –85°C before being slowly warmed to room temperature over the next 2 d. The samples were then washed three times in acetone followed by gradual infiltration in Spurr's resin (Spurr 1969). Thin (70 nm) sections were cut from pellets of both the benthic cell and flagellate preparations using a Leica UC7 ultramicrotome (Leica Microsystems) and poststained with 1% aqueous uranyl acetate and triple lead stain (Hanaichi et al. 1986). The sections were imaged using a Tecnai Spirit transmission electron microscope (Thermo Fisher Scientific) equipped with an Eagle 2 K CCD camera.

Molecular phylogenetics. Total genomic DNA was extracted using a modified CTAB protocol (Cremen et al. 2016). The 18S rRNA gene was amplified and sequenced using universal primers eukAF (5'-AAYCTGGTTGATCCTGCCAG-3')/eukBR (5'-GATCCWCTGCAGGTTACCTA-3') or newly developed pelagophyte specific primers PeIF(5'-ATACCCGTAGTAATTCTAGAGC-3')/PeIR(5'-CCATGCTAATGTATTCAAGGC-3'), and followed a thermocycling regime consisting of an initial

temperature of 94°C for 2 min; 40 cycles of 94°C for 30 s, 52°C for 30 s, and 72°C for 2 min; and a final elongation step of 72°C for 5 min. Forward and reverse reads were assembled and edited using Geneious Prime v.2019.2.3 (Kearse et al. 2012). For high-throughput sequencing, extracted DNA was sent to GENEWIZ (Suzhou, China), where libraries were generated using the Illumina VAHTS Universal DNA Library prep kit and protocols, and sequenced on the NovaSeq System (paired-end, 150 bp reads, ~4 Gb of data).

Recent phylogenies for pelagophytes have used six genes: the nuclear 18S rRNA gene, and the plastid genes *psaA*, *psaB*, *psbA*, *psbC* and *rbcL* (Han et al. 2018, Wetherbee et al. 2021). To obtain these plastid genes, the Illumina data were assembled (Marcelino et al. 2016, Jackson et al. 2018) and chloroplast contigs annotated (Cremen et al. 2018, 2019) as previously described, and the relevant genes extracted from the assembly. Sequences of 18S rRNA and the five chloroplast markers were submitted to GenBank (Table S1). We downloaded additional sequences of the same six genes from representatives across the pelagophyte tree of life as well as diatoms, bolidophytes and Dictyochophyceae as outgroups (Han et al. 2018; Table S1). Sequences were aligned for each gene with TranslatorX v.1.1 (Abascal et al. 2010), using Muscle v3.8.31 as the alignment algorithm (Edgar 2004). Following a visual check of the alignments, they were concatenated and the resulting supermatrix analyzed with maximum likelihood (ML) searches in RAxML v.8.2.12 (Stamatakis 2014) using the GTR + Gamma model and using 25 randomized MP starting trees. Branch support was obtained by running 100 standard bootstrap replicates.

An additional 18S-only tree was inferred to see the placement of an additional genus (*Chrysophaeum taylorii*: MK088058) and the sequences of some unnamed culture strains (CCMP2097: EU247837; CCMP2135: KF899841; RCC2040: JF794050), for which the plastid genes are not available. This tree was inferred with RAxML using a GTRGAMMA model and 1000 rapid bootstraps.

To investigate the evolution of the PT, we created an uncalibrated chronogram using the correlated model implemented in the chronos function of the ape package (v.5.6-2) in R v.4.2.1 (Sanderson 2002, Popescu et al. 2012, R Core Team 2021). We inferred the evolution of the extent of the PT among pelagophyte taxa, data for the number of PT layers and the total PT thickness were compiled per genus. The chronogram was trimmed down to those genera for which data was available and ancestral state estimation carried out for the number of PT layers using an equal-rates Markov model using the make.simmap function in phytools (100 simulations) and for the PT thickness using a Brownian motion model with the contMap function in phytools v.1.0-3 (Revell 2012).

RESULTS

Species descriptions. Based on a combination of morphological observations and our phylogenetic results, we describe three new genera and species (Fig. 1).

***Wyeophycus julieharrissiae* Wetherbee, gen. et sp. nov. (Figs. 2–5)**

Description – Marine, unicellular thalli; alternated between a sand-dwelling benthic stage and a short-lived heterokont flagellate stage; strongly adhered benthic cells somewhat flattened on the surface, oblong (8–10 µm long, 4–6 µm wide) to rounded

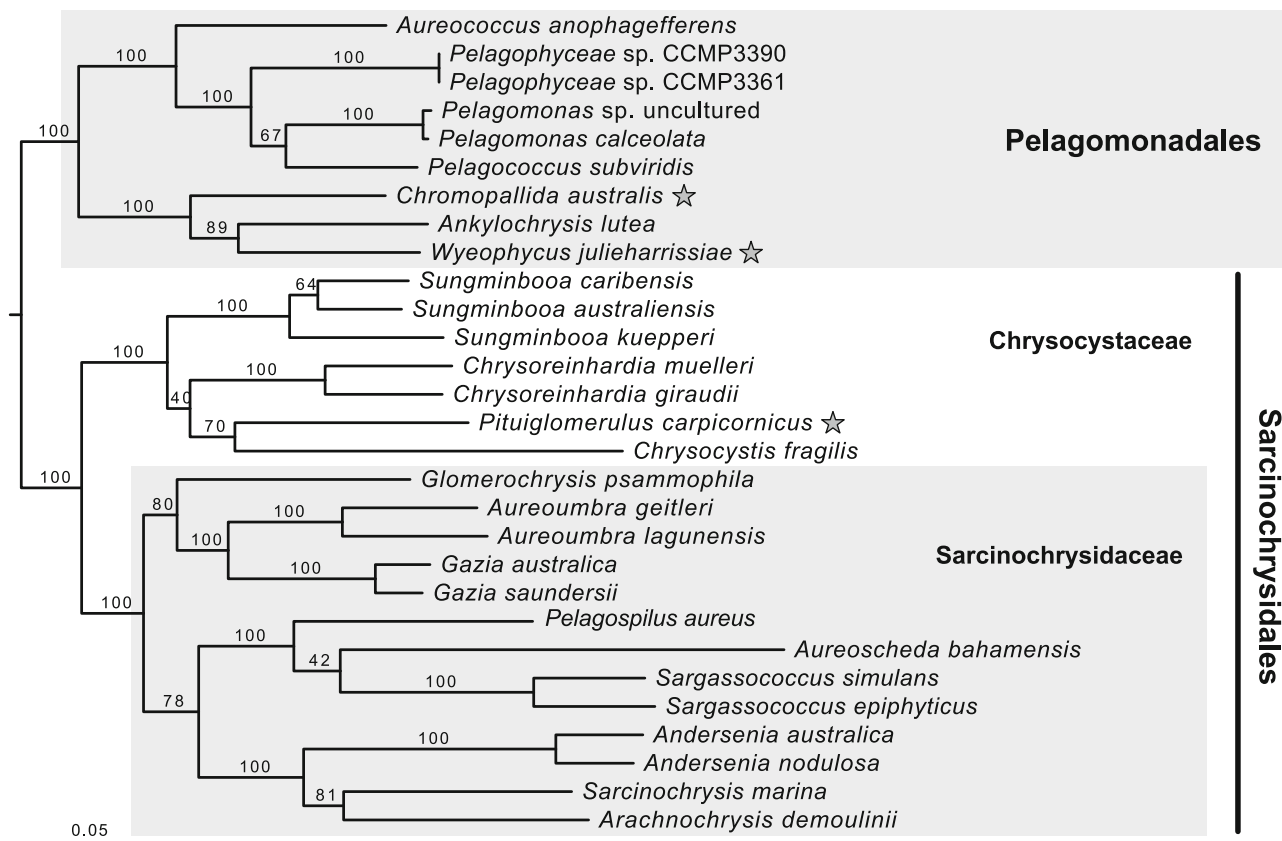


FIG. 1. Maximum likelihood tree showing the phylogenetic position of the three newly described species (indicated by stars) among the pelagophytes based on an alignment of 18S rRNA and five plastid genes (*psaA*, *psaB*, *psbA*, *psbC*, *rbcl*). Numbers on the branches show bootstrap support and the scale bar indicates estimated substitutions per site.

(6–10 μm in diameter); two short flagella (4–6 μm in length) were observed on most benthic cells, emerging from a subapical pit on the ventral surface; flagella stationary, only beat when cells released from the substratum and became briefly motile, settled and adhered in a new position; large chloroplast with two lobes, highly fenestrated with multiple pyrenoids in parallel sheets extended the entire length of each lobe; a large compartment of grainy cytoplasm was located at the posterior of cells; benthic cells shed their PT prior to cell division, daughter cells either flatten out and remained benthic, or developed into ovoid zoospores (6–8 μm long, 4–5 μm wide) with two short heterokont flagella (both 4–6 μm in length) that propel the flagellates in a fluttering, spinning motion; transmission electron microscopy showed cells surrounded by a 5-layered PT derived from rafts in vesicles that develop within the cytoplasm; nuclear encoded 18S rDNA and plastid encoded *rbcl*, *psaA*, *psaB*, *psbA* and *psbC* sequences distinctive from those of other pelagophytes, with GenBank accessions of reference sequences listed in Table S1.

Holotype – MELU A Wye36, a mounted specimen derived from strain CS-1474, collected from sand in

a large, deep tide pool, by R. Wetherbee in April 2016.

Type locality – Deep tide pool, Wye River (Wye36), Victoria (38°38'20" S; 143°53'34" E).

Etymology – *Wyeophycus* refers to an alga from Wye River where it was collected. The specific epithet *W. julieharrissiae* refers to Julie Harris-Wetherbee who supported and made possible all the work of the first author for over 40 years.

Habitat – marine, sand-dwelling.

Culture lodgement – ANACC code: Wye36, Victoria strain CS-1474, CSIRO, Hobart, Tasmania, Australia.

***Chromopallida australis* Wetherbee, gen. et sp. nov. (Figs. 6 and 7)**

Description – Marine, unicellular flagellate; cells bean shaped, 5–7 μm long, 4–5 μm wide; heterokont flagella arise from a subapical depression on the ventral surface of the cell, 1/3 the distance from the cell apex; the long, forward projecting flagellum (#2) with mastigonemes is slightly longer than the cell, 9–12 μm , while the short, smooth flagellum (#1) is the same length as the cell, 5–7 μm ; a single, slender and tubular chloroplast is pale golden-green, extending the length of the cell, curved sharply at each end; a single pyrenoid is embedded in the chloroplast, cells covered by a 4-layered, PT plus

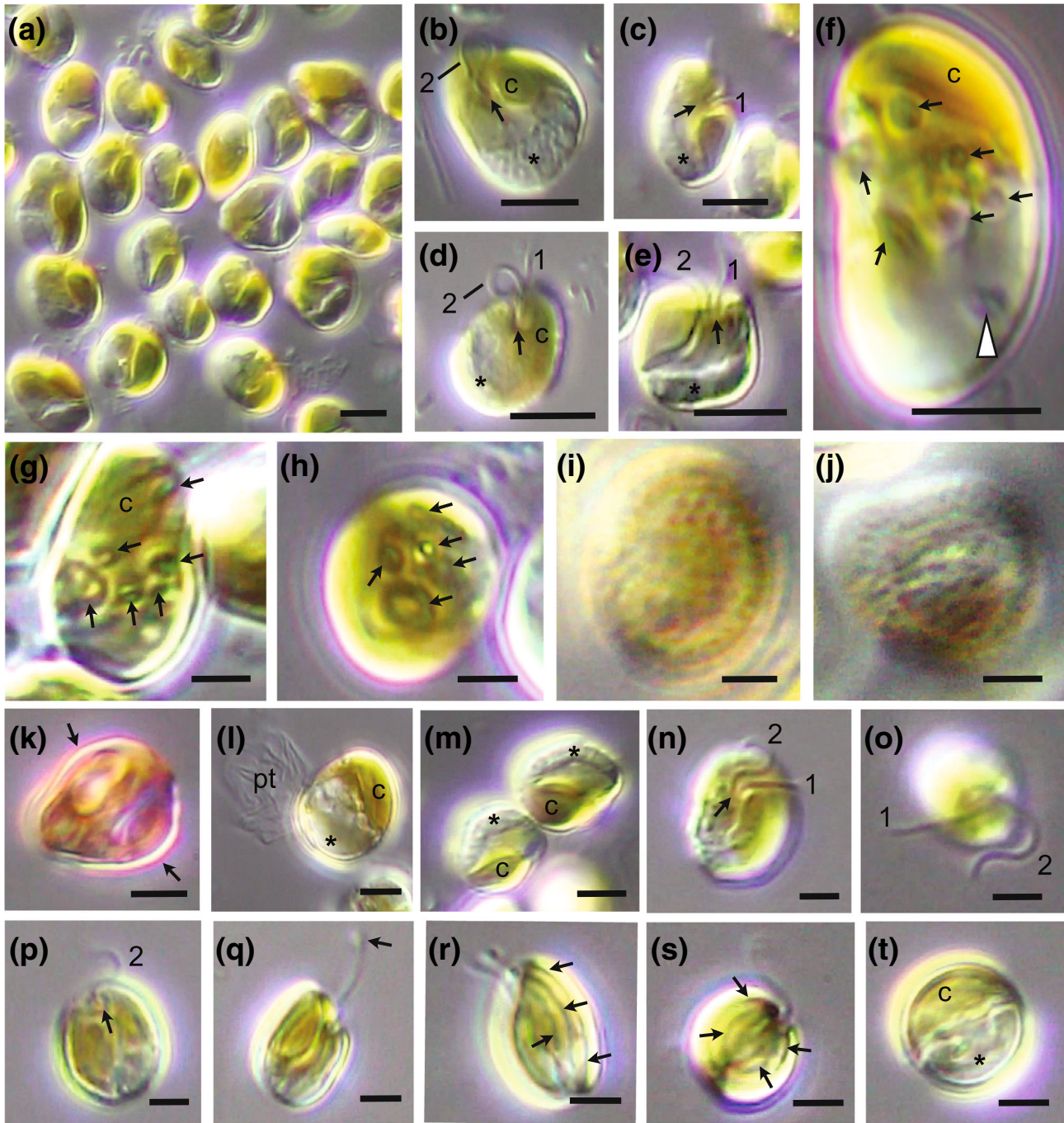


FIG. 2. Light microscopy of *Wyeophycus julieharriissiae* gen. et sp. nov. (a–e) Benthic cells were oblong (8–10 μm long, 4–6 μm wide) to rounded (6–8 μm in diameter) and flattened on the substratum, the ventral surfaces exposed with the two lobes of the chloroplast (c) at the apical end of cells while a compartment of grainy cytoplasm was at the cell posterior (asterisk, b–e). High magnification of benthic cells showed the subapical pit where two short, heterokont flagella emerged (arrows, b–e), the immature flagellum (2) typically bent forward as it exited the cell (b, d) while the mature flagellum (1) was straight or bent towards the posterior of the cell (c, e). (f–h) High magnification of benthic cells prior to division showed the presence of large, donut-shaped vesicles (“PT vesicles”) of varying size that accumulated in pockets of the chloroplast lobes and near the cell surface (see below, Figs. 3 and 4). (i–k) When stained with toluidine blue the surface of benthic cells showed lumps, the PT staining pink to purple (arrows). (l) A benthic cell showed one lobe of the chloroplast (c) and the posterior grainy compartment of cytoplasm (asterisk) and had shed its PT (pt) prior to division. (m) Benthic daughter cells (4–6 μm long, 4 μm wide) following recent division. (n–p) Oblong daughter cells released from the substratum as heterokont zoospores (6–7 μm long, 4–5 μm wide) with short heterokont flagella (mature flagellum 1, immature flagellum 2, both c. 4.0 μm long) emerging from a subapical pit (arrows) as described above for benthic cells. (q–t) Zoospores adhered to a surface first with the tip of their #2 flagellum (arrow, q), the cells then adhered and flatten out (r–t). Note the layered pyrenoids seen within the zoospore chloroplast in longitudinal and cross-section (arrows, r, s). Scale bars = 5 μm (a–f), 2 μm (g–t).

wall layers; nuclear encoded 18S rDNA and plastid encoded *rbcL*, *psaA*, *psaB*, *psbA* and *psbC* sequences distinctive from other pelagophytes, with GenBank accessions of reference sequences listed in Table S1.

Holotype – MELU A #Och39, a mounted specimen derived from strain CS-1472, collected from a tide pool by B. Grant in January 2009.

Type locality – Intertidal pool, Trial Bay (Och39), Tasmania, Australia (43°07'054" S; 147°15'019" E),

Etymology – *Chromopallida* refers to the “golden-green, somewhat pale” color of the cells, while the specific epithet, *C. australis* refers to the country the species was found in.

Habitat – marine, planktonic flagellate.

Culture lodgement – ANACC code: Och39, Victoria strain CS-1472, CSIRO, Hobart, Tasmania, Australia.

***Pituiglomerulus capricornicus* Wetherbee, gen. et sp. nov. (Figs. 6 and 8)**

Description – Marine, benthic; colonial organisms; clusters of colonies comprised of sarcinoid packets, typically containing 4, 8 or 16 closely packed cells surrounded by 1–3 gelatinous sheaths; clusters embedded in large quantities of adhesive mucilage that adheres to the substratum (e.g., sand); cells spherical, 8–9 µm in diameter prior to division, divide twice to produce four imbricated cells in compact colonies also 8–9 µm in diameter; individual cells oblong, 3 × 5 µm; one deeply lobed, fenestrated chloroplast dominated the cytoplasm; protruding stalked pyrenoid(s); cells surrounded by a thin, PT with distinct pores when viewed with transmission electron microscopy, a cell wall and mucilage layers; vegetative colonial reproduction by cluster fragmentation; zoospores not observed in cultures; nuclear encoded 18S rDNA and plastid encoded *rbcL*, *psaA*, *psaB*, *psbA* and *psbC* sequences distinctive from other pelagophytes, with GenBank accessions of reference sequences listed in Table S1.

Holotype – MELU A #HI 1, a mounted specimen derived from strain CS-1473, collected from sand in a large lagoon, by M. Pasella in February 2020.

Type locality – Lagoon sand, Heron Island (HI 1), Queensland, Australia (23°26'38.1" S; 151°54'55.0" E).

Etymology – *Pituiglomerulus* (pitui = slime or phlegm) refers to the slimy cluster of colonies, while the specific epithet, *P. capricornicus* refers to the Capricorn group of reefs that includes Heron Island where the species was found.

Habitat – marine, sand-dwelling.

Culture lodgement – ANACC code: HI 1, Queensland strain CS-1473, CSIRO, Hobart, Tasmania, Australia.

Molecular phylogeny. The phylogenetic tree recovered the principal groups of Pelagophyceae (Fig. 1), including a basal split between the Pelagomonadales and Sarcinochrysidales as well as the two families within the latter. The newly described organisms *Chromopallida australis* and *Wyeophycus julieharrissiae* are placed confidently in the Pelagomonadales, forming a well-supported lineage with *Ankylochrysis lutea*. The new taxon *Pituiglomerulus capricornicus* is a

deep-branching lineage within the Chrysocystaceae. Bootstrap values of 70 for the branch joining *Chrysocystis* and *Pituiglomerulus* as sisters and 40 for the branch subtending these two taxa and *Chrysoreinhardia* indicate substantial uncertainty in the exact relationships among the genera of Chrysocystaceae (Fig. 1).

The 18S rDNA gene phylogeny (Fig. S1) had relatively low support compared to the six-gene phylogeny but showed the placement of *Chrysophaeum* as sister to remaining Chrysocystaceae and of strains CCMP2097 and RCC2040 within the same lineage as *Wyeophycus*, *Chromopallida* and *Ankylochrysis* in the Pelagomonadales but distinct from the new genera *Wyeophycus* and *Chromopallida*.

Observations for Wyeophycus julieharrissiae. *Light microscope observations:* Species is unicellular, alternating between a sand-dwelling, dominant benthic stage where cell division occurs (Fig. 2, a–m) and a short-lived, heterokont flagellate stage with very short flagella (Fig. 2, n–t). Benthic cells were slightly flattened and adhered to the substratum, oblong to rounded, (Fig. 2, a–f). A single, bilobed chloroplast (c) dominated the cytoplasm in the apical region of the cell while the cell posterior was dominated by a compartment of grainy cytoplasm (asterisk, Fig. 2, b–e). Two short heterokont flagella emerged from a subapical pit located on the ventral surface approximately 1/3 from the cell apex (arrows, Fig. 2, b–e). Flagella were 4–6 µm in length, barely extending into the surrounding medium, the #2 (immature) flagellum often with one sigmoid curve, while the #1 (mature) flagellum was straight or bent in a posterior direction (Fig. 2, b–e). The flagella of benthic cells were typically still and difficult to observe, in which case the cells were strongly adhered to the substratum. Alternatively, flagella were slowly beating and those cells were slightly shaking and only loosely adhered. Benthic cells occasionally released from the surface and became briefly motile, the short flagella beating in a way that caused the cells to flutter and spin over the surface before quickly settling and adhering once again. In the time period leading up to division, just after the lights came on, pockets of cytoplasm in the fenestrated chloroplast lobes were observed and contained donut-shaped vesicles (termed PT vesicles; Fig. 2, f–h) that appeared to be involved in the formation and secretion of multilayered PT rafts (see TEM observations below). Lumps often appeared on the surface of flattened, rounded benthic cells, the covering stained pink to purple with toluidine blue (Fig. 2, i–k).

Only benthic cells were observed to divide, the parental cell shedding the PT just prior to division (Fig. 2l), daughter cells either remaining benthic (Fig. 2m) or forming zoospores and releasing from the substratum (Fig. 2, n–p) where they were motile for a few minutes before settling and re-establishing the benthic stage (Fig. 2, q–t). As stated above, benthic cells can transform into flagellates without

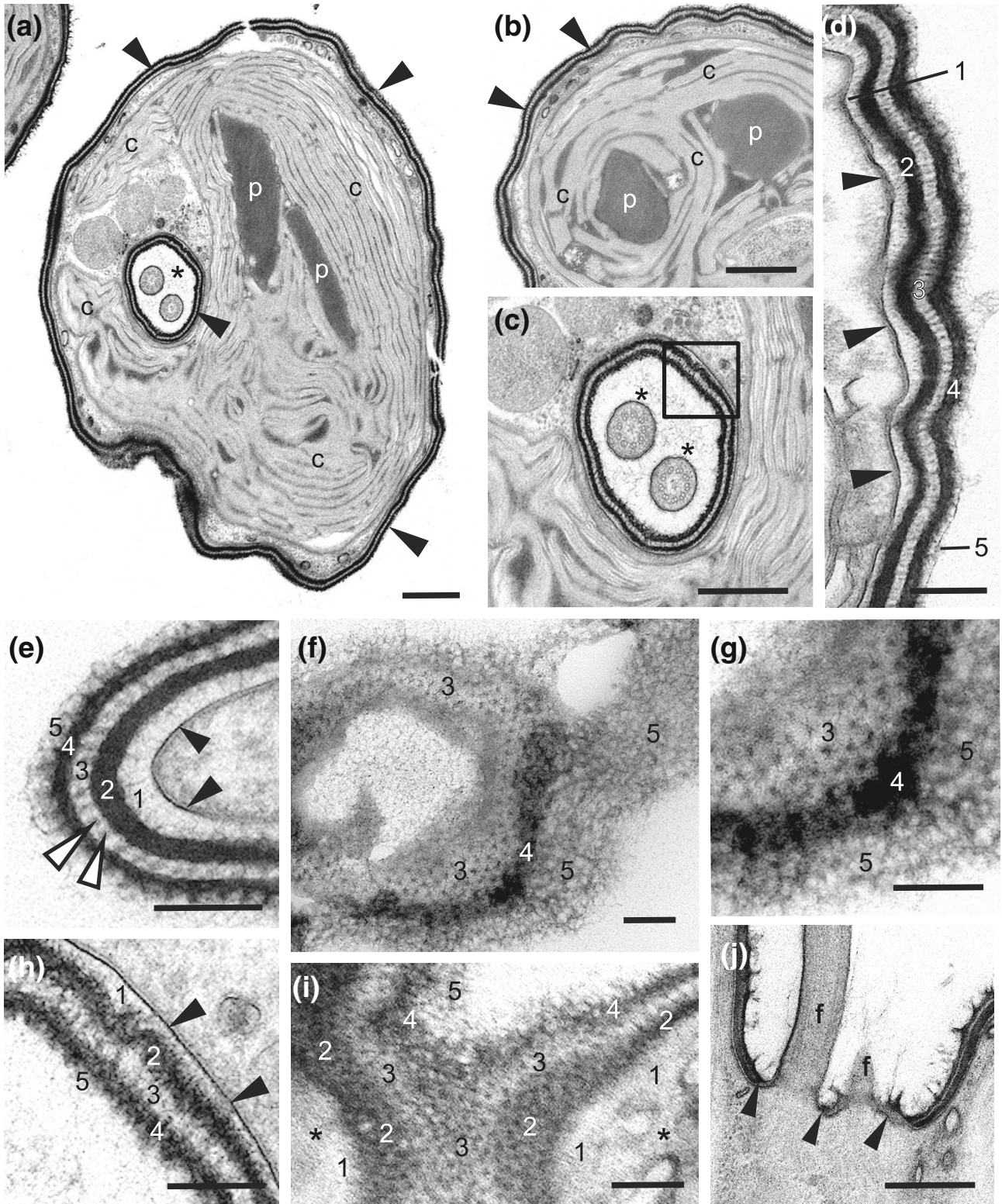
division, and in that case are normally larger in size. Zoospores, representing the flagellate stage were bean shaped, approximately 6 μm long, 4 μm wide with short flagella emerging from a shallow pit on the ventral surface (Fig. 2, o–p) as described above for benthic cells (Fig. 2, b–e). Motile zoospores were observed to flutter and spin over the surface, the exact action of the two short flagella was difficult to observe. A single flagellum adhered to the substratum (arrow, Fig. 2q) before cells adhered to the surface and rounded up (Fig. 2t). Each daughter cell contained a single lobe of the parental chloroplast and revealed multiple embedded pyrenoids in a uniform alignment (Fig. 2, r and s).

Fine structure. The HPF fixation of *Wyeophycus julieharrissiae* was excellent for most components (Figs. 3–5). Lobes of the chloroplast dominated the apical end of cells and multiple pyrenoids were observed embedded in the lobes (Fig. 3, a and b). An extracellular, multilayered cell covering, termed a PT covered the cell surface (Fig. 3, a–j), including the subapical flagella pit (Fig. 3, a and c), except where basal bodies/flagella were positioned (Fig. 3j). The plasma membrane (PM) was 10–12 nm thick and the outer surface was distinctly thicker and more electron dense (black arrowheads, Fig. 3, e and h). The complex PT undulates over the surface and was comprised of 5 layers (Fig. 3, c and i) that were distinctive in both cross and tangential sections. In cross-section from the PM outward, layer #1 (25–30 nm) was lightly stained and fibrous with some fibers running perpendicular between the PM and layer #2 (best seen in Fig. 3d). Layers #2 and #4 were electron dense (c. 20–30 nm in width) and perforated with small pores (10–12 nm in diameter - best seen in Fig. 3h), and sandwich layer #3 (20–25 nm) that was characterized by equally spaced columns (20–25 nm between) with swollen central regions (white arrowheads, Fig. 3e) that define large pores (20–25 nm in diameter) in a honeycomb construction when observed in tangential sections through layers 3–5 (Fig. 3, f and g) and layers 1–5 (Fig. 3i). Note that the honeycomb structure was observed in layer 2 as well as layer 3 (Fig. 3i), but the electron density of layer 2 normally hid this feature. Layer 5 (20 nm plus) varied in thickness and was less opaque than layer 4, (Fig. 3, d–i) while both layers had irregularly shaped pores ranging in size from 15 to 20 nm in diameter (Fig. 3, f, g and i). Layer 5 often

developed elongated extension in older, predivision benthic cells, increasing the overall thickness of the PT (e.g., Fig. 3j).

Two or more, large Golgi stacks were observed within the cytoplasm, the forming faces adjacent to the nucleus (e.g., Fig. 4a). As benthic cells shed the parental PT prior to division (Fig. 2l), they must have first produced a new PT for the daughter cells as no naked cells were ever observed. Cells fixed in this stage of the cell cycle contained a range of vesicles that extended out from the distal, mature face of the Golgi into the cytoplasm, many vesicles contained the same precisely layered components observed in the PT (Fig. 4, a–l). Vesicles of all sizes and shapes accumulated in pockets within the chloroplast lobes (asterisk, Fig. 4, b–d), many larger vesicles, termed “PT vesicles”, contained segments or “rafts” of the PT in various orientations. Other vesicles closer to the Golgi were multilayered, or membrane-bound vesicles within membrane-bound vesicles. Images suggest either the invagination of the vesicle membrane to form more compartments (e.g., Fig. 4e), or by the uptake of adjacent whole vesicles to form multilayered vesicles (best images are from other pelagophytes; see below). PT vesicles were enlarged in the chloroplast pockets and the contents took on the detailed features of the PT, for example the honeycomb structure of layer 3 sandwiched between two electron dense layers (Fig. 4, b and h). Apparently fully formed PT vesicles were observed, often adjacent to the PM (Fig. 4, i and j). Starting with the vesicle membrane and proceeding inward (Fig. 4, i and l), PT layers 1–4 were observed with layers 2, 3 and 4 being the most obvious, particularly the honeycomb structure of layer 3 seen in glancing section of some vesicles (e.g., Fig. 4, b and h). Layer #5 was less obvious. In cross-section, mature PT rafts were observed to be U-shaped, but only slightly opened at the end (Fig. 4, k and l), the site where images suggest the PT vesicles might fuse with the PM and add a raft to an enlarging PT (Fig. 4, m and o). Sites of raft secretion were seen in the middle of cells, near chloroplast lobes, and discontinuities often appeared where the inclusion of rafts did not appear to fit perfectly (arrow, Fig. 4, n and o). Benthic cells often have an undulating surface (Fig. 5a), which may account for the appearance of lumps seen in light microscope images (Fig. 2, i and j).

FIG. 3. Fine structure of *Wyeophycus julieharrissiae* gen. et sp. nov. (a, b) Chloroplast lobes (c) dominated the cytoplasm in the apical half of the cell including embedded pyrenoids (p). A multilayered PT (arrowheads) covered the cell surface, which included the flagella pit (asterisk) with two flagella in cross-section. (c) Flagella pit region in Figure 2a showed the PT and flagellar cross-sections (asterisks) in more detail. (d, e) High magnification images of the 5 layers of the extracellular PT (1–5) in cross-section numbered out from the plasma membrane (black arrowheads). The surface often undulated. Note the swollen regions of the columns in layer 3 (white arrowheads). (f, g) Glancing sections through layers 3–5 showed the honeycomb structure of layer 3 and the pores in layers 4 and 5. (h) High magnification of boxed region of 3c, showed the porous nature of layers 2 and 4. (i) High magnification of a glancing section showed the porous layers 3–5. (j) Longitudinal section through the flagellar pit where two flagella emerged. The PT (arrowheads) was continuous except where the flagella (f) emerge. Scale bars = 0.5 μm (a–c, j), 100 nm (d–i).



The PM in glancing structure appears as a distinctive strap and may have an outer surface layer that is more densely stained (arrowhead, Fig. 5a, and in cross-section, Fig. 3, e and h).

Golgi stacks were observed in cells at all stages of the cell cycle, but large PT vesicles were only observed by light microscopy in cells 2–3 h just before and during the division cycle. Golgi appear

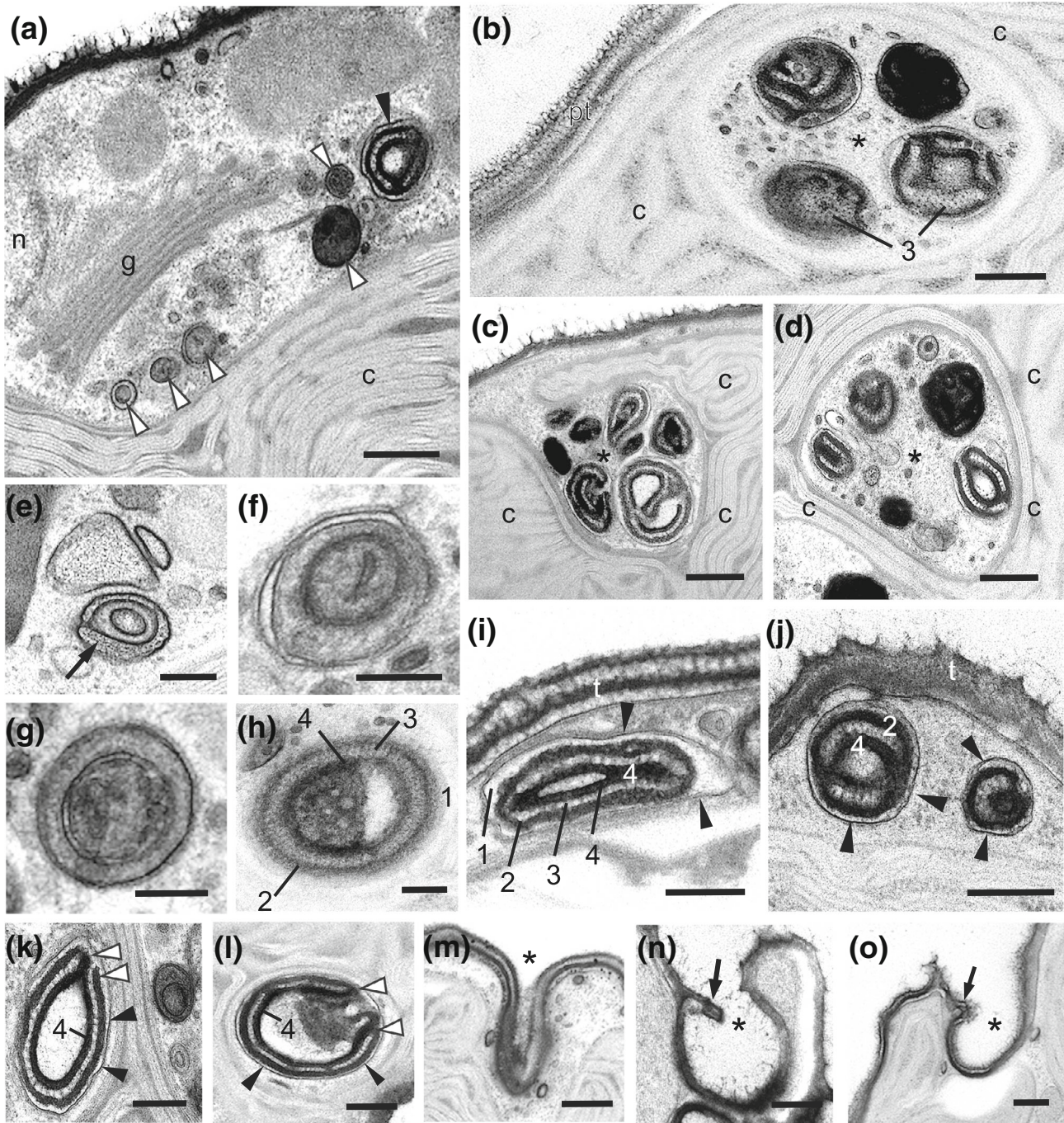


FIG. 4. Fine structure of *Wyeophycus julieharriissiae* gen. et sp. nov. (a) Golgi stack (g), the forming face adjacent the nucleus (n) and vesicles of various morphology were observed near the distal face of the Golgi (white arrowheads), including a larger PT vesicle (black arrowhead) with contents constructed like the layers of the PT. (b–d) Pockets of cytoplasm (asterisk) in the chloroplast (c) contained PT vesicles with contents that showed the same layered structure observed in the PT covering. Note the honeycomb morphology in glancing sections of layer 3 (e.g., b). (e–h) Multilayered cytoplasmic vesicles observed near Golgi stacks with various morphologies, the larger vesicles taking on the layered structure (layers 2–4) of PT segments or rafts. (i–h) Multilayered cytoplasmic vesicles observed near Golgi stacks with various morphologies, the larger vesicles taking on the layered structure (layers 2–4) of PT segments or rafts. (i, j) PT vesicles surrounded by their membrane (arrowheads) and slightly open at one end (white arrowheads). (k, l). Large PT rafts surrounded by a membrane (black arrowheads) and slightly open at one end (white arrowheads). (m–o) Stages where PT rafts have fused with the PT (asterisk), often appearing to disrupt the continuity of the PT (arrows). Scale bars = 200 nm (a, k–o), 100 nm (b, f, g, j–l), 0.5 μ m (c, d), 1.0 μ m (e), 40 nm (h, i).

to be pumping out a range of vesicles with different content, some multilayered and others not (Fig. 5b). Vesicles are observed to accumulate

beneath the PM (Fig. 5, b and c), and also in the extracellular space between the PM and layer 2 of the PT where they appear to be in stages of

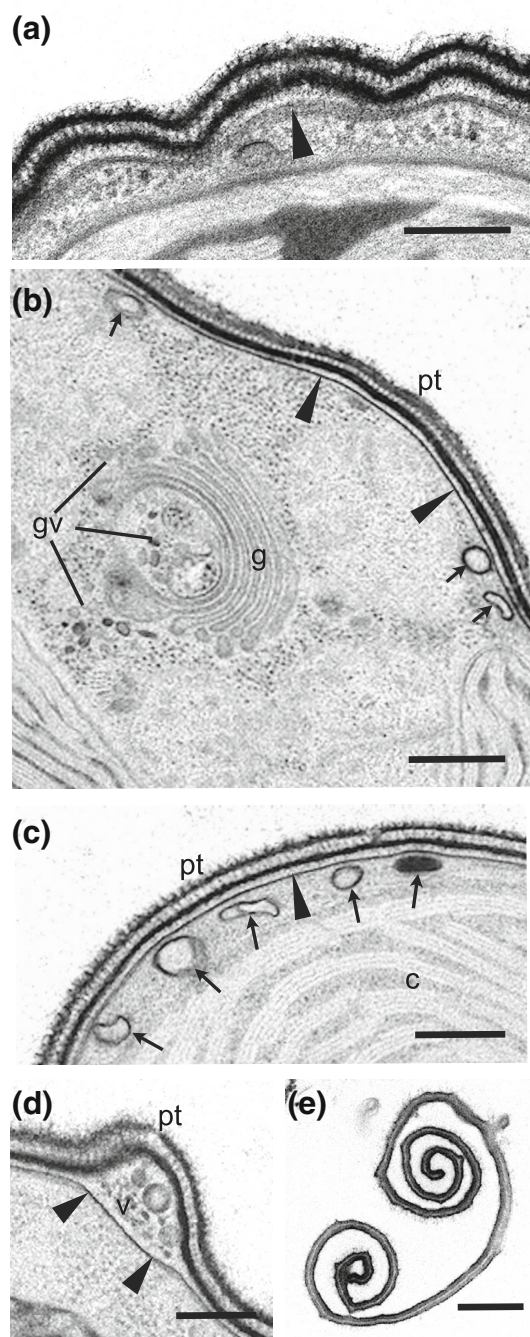


FIG. 5. Fine structure of *Wyephyucus julieharrissiae* gen. et sp. nov. (a) Undulated surface of mature benthic cells. The PM in glancing section appeared as a recognizable band (arrowhead). (b) Large Golgi stack (g) with arrays of small Golgi-derived vesicles (gv) of varying morphology, some vesicles (arrows) positioned adjacent the PM (arrowheads) and overlying PT. (c) Vesicles (arrows) underlie the PM (arrowheads) and PT. (d) Small extracellular vesicles (v) occasionally occupy layer #1 of the PT, just outside the PM (arrowhead). (e) Section through a shed PT that were common in TEM pellets of recently divided cells. Scale bars = 100 nm (a), 200 nm (b–d), 0.5 μ m (e).

disintegration (Fig. 5d). The PT is shed prior to division, and their remains are common in sections (Fig. 5e).

Observations for Chromopallida australis. *Light microscope observations:* Isolated from seawater in a sample collected with tide pool sand, this species was a planktonic, unicellular flagellate (Fig. 6, a–f) and was never observed adhered to the substratum like *Wyephyucus julieharrissiae* (Fig. 2, a–m) and *Pituiglomerulus capricornicus* (Fig. 6, g–o). Flagellates were oval to bean shaped, 5–7 μ m long and 4–5 μ m wide, and very lightly pigmented. Thick cultures of *Chromopallida australis* were virtually colorless, as cells have only a single, pale, golden brown chloroplast. The chloroplast was tubular, running the length of the cell, curved sharply at each end (Fig. 6, a–c), and contained an embedded pyrenoid. A large storage vesicle of unknown composition was observed near the middle of the cell (Fig. 6e). The chloroplast was observed to replicate prior to cell division. Two unequal, heterokont flagella arose on the ventral cell surface in a depression about one-third to half the length of the cell from the apex (Fig. 6, a and f). The anterior, immature long flagellum (#2) was longer than the cell (10–14 μ m) while the short flagellum (mature #1) was the same length as the cell (5–7 μ m). The nucleus was located below the basal bodies and two storage vesicles (chrysolaminarin?) were normally present at opposite ends of the cell (Fig. 6, c and e).

Fine structure. The HPF fixation of this species was good enough to see the key cytoplasmic organelles and features of the PT (Fig. 7, a–o). Cells had a central nucleus (n) and a chloroplast running along one edge of the cells with a number of storage vesicles (s) of various morphology and a mitochondrion (Fig. 7, a and c). The PM-PT at low magnification appeared together as one electron dense covering (Fig. 7a). Two morphologically different types of Golgi dominated the cytoplasm, smaller stacks (c. 0.4–0.5 μ m in diameter) with electron dense contents making them stand out (Fig. 7, b and f). The cisternal contents appeared porous and displayed tiny pores (10–12 nm in diameter) in the correct orientation (Fig. 7f). The small Golgi were typically adjacent to one another, the forming faces abutting a nucleus (Fig. 7, b and d). The second type of Golgi was larger (1.0–1.2 μ m in diameter) with 15–20 cisternae in a stack and did not have electron dense contents, but were multilayered (Fig. 7, d, g and h). The extracellular PT was comprised of 4 layers (Fig. 7, i and n), layers 1 and 3 were thin and fibrous and varied in thickness (c. 20–30 nm), while layers 2 (50–60 nm thick) and 4 (25–35 nm thick) were electron dense and perforated. Layer 4 often produced fibrous projections of various length (up to 100+ nm) off the surface (Fig. 7d). The porous construction was best seen in glancing sections (Fig. 7, j and m), and consisted of two types of pores, mainly micropores (10–12 nm in diameter) plus the occasional macropore (20–22 nm in diameter; Fig. 7, l–n) that only penetrated layer 2 as seen in cross-section (Fig. 7n).

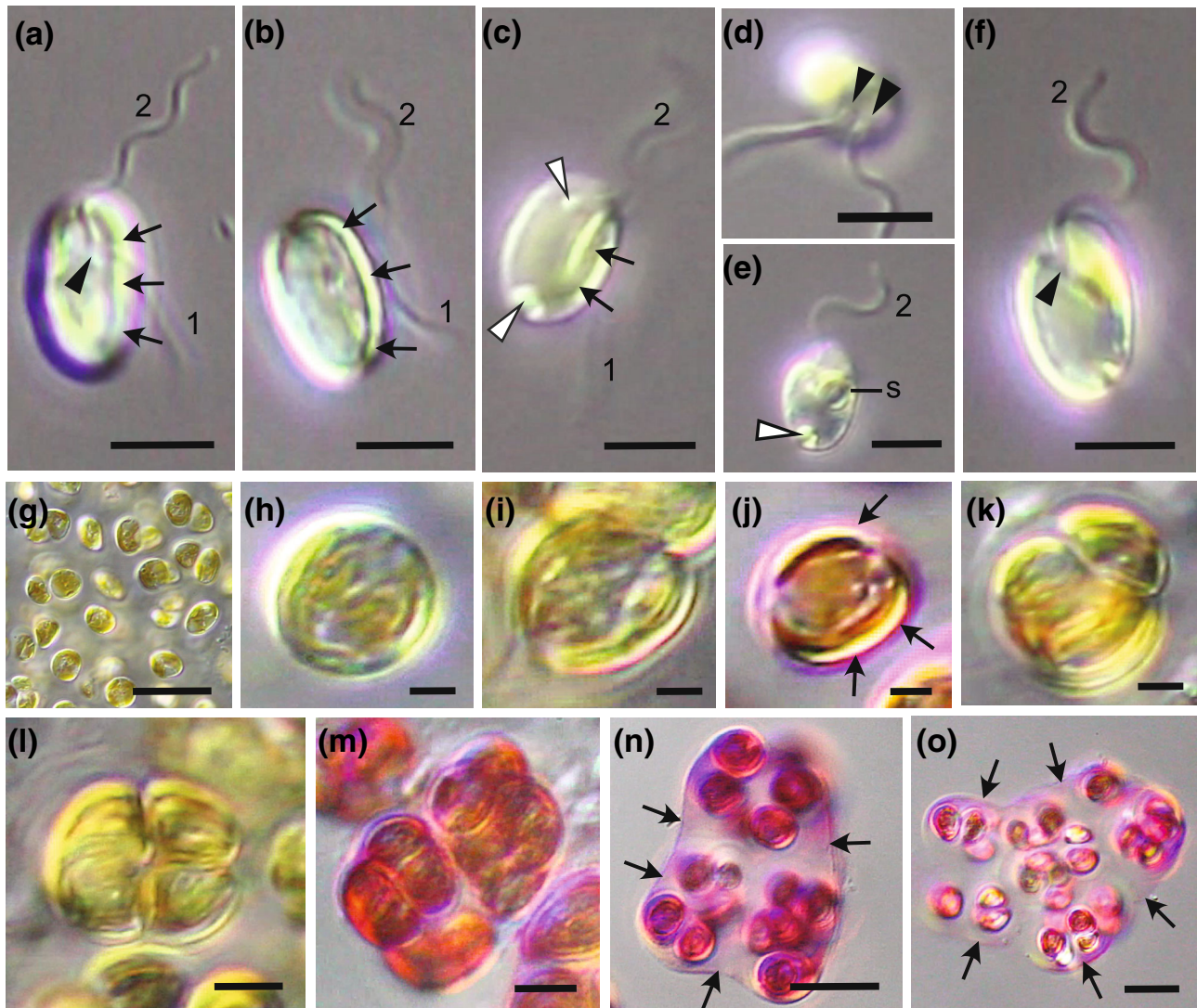


FIG. 6. Light microscope observations of *Chromopallida australis* gen. et sp. nov. (a–f) and *Pituiglomerulus capricornicus* gen. et sp. nov. (g–o). *C. australis*. (a, b) Unicellular flagellates oblong to bean shaped with heterokont flagella (immature 2, mature 1) that emerged subapically (black arrowhead) from a shallow depression or vestibulum on the ventral surface of the cell. A narrow, tubular, chloroplast ran the length of the cell, curved at both ends (arrows). (c) Ventral surface of a cell showing the chloroplast (arrows) and a storage vesicle at the posterior tip of cell (white arrowhead). (d) Two flagella (arrowheads) emerged at the cell apex from a depression (arrowheads). (e) A large storage vesicle (s) appeared near the center of the cell as well as the storage vesicle at the cell posterior (arrowhead). (f) Side view of the immature flagellum (2) that emerged from a depression or vestibulum (arrowhead). *P. capricornicus*. (g) Individual cells embedded in mucilage prior to a division cycle. (h, i) Cells contained a highly fenestrated chloroplast. (j) Cell stained with toluidine blue with a pink to purple PT/cell wall. (k) Following 2 division cycles, daughter cells were tightly imbricated, the resulting four celled clusters were initially the same diameter as single cells. (l) Cells enlarged and separated as further divisions occurred. (m–o). Cells surrounded by cell walls, gel sheaths and mucilage stained with toluidine blue. (m) Clusters of cells in sarcinoid packs of 4, 8, 16 were surrounded by a series of mother cell walls, grandmother cell walls, great grandmother cell walls, etc. (n, o) Clusters started to grow apart from one another, then cell packets separated into single cells (see g), all engulfed by a lightly stained mucilage (arrows). Scale bars = 4 μm (a–f), 20 μm (g), 2 μm (h–k), 5 μm (l, m), 10 μm (n, o).

Extracellular, membrane-bound vesicles were observed between the PM and layer 2 of the PT (Fig. 7o), and often appeared in a state of disintegration.

Observations for *Pituiglomerulus capricornicus*. *Light microscope observations:* A marine, benthic, sand-dwelling species comprised of clusters of spherical cells 8–9 μm in diameter widely separated by large

quantities of mucilage prior to a division cycle (Fig. 6, g–i). One deeply lobed, fenestrated chloroplast dominated the cytoplasm (Fig. 6, h and i) with protruding, stalked pyrenoids that were best seen in transmission electron microscopy. Cells divided twice to produce four imbricated cells in compact colonies also 8–9 μm in diameter (Fig. 6, k and l); individual cells oblong, 3 \times 5 μm in size before expanding and

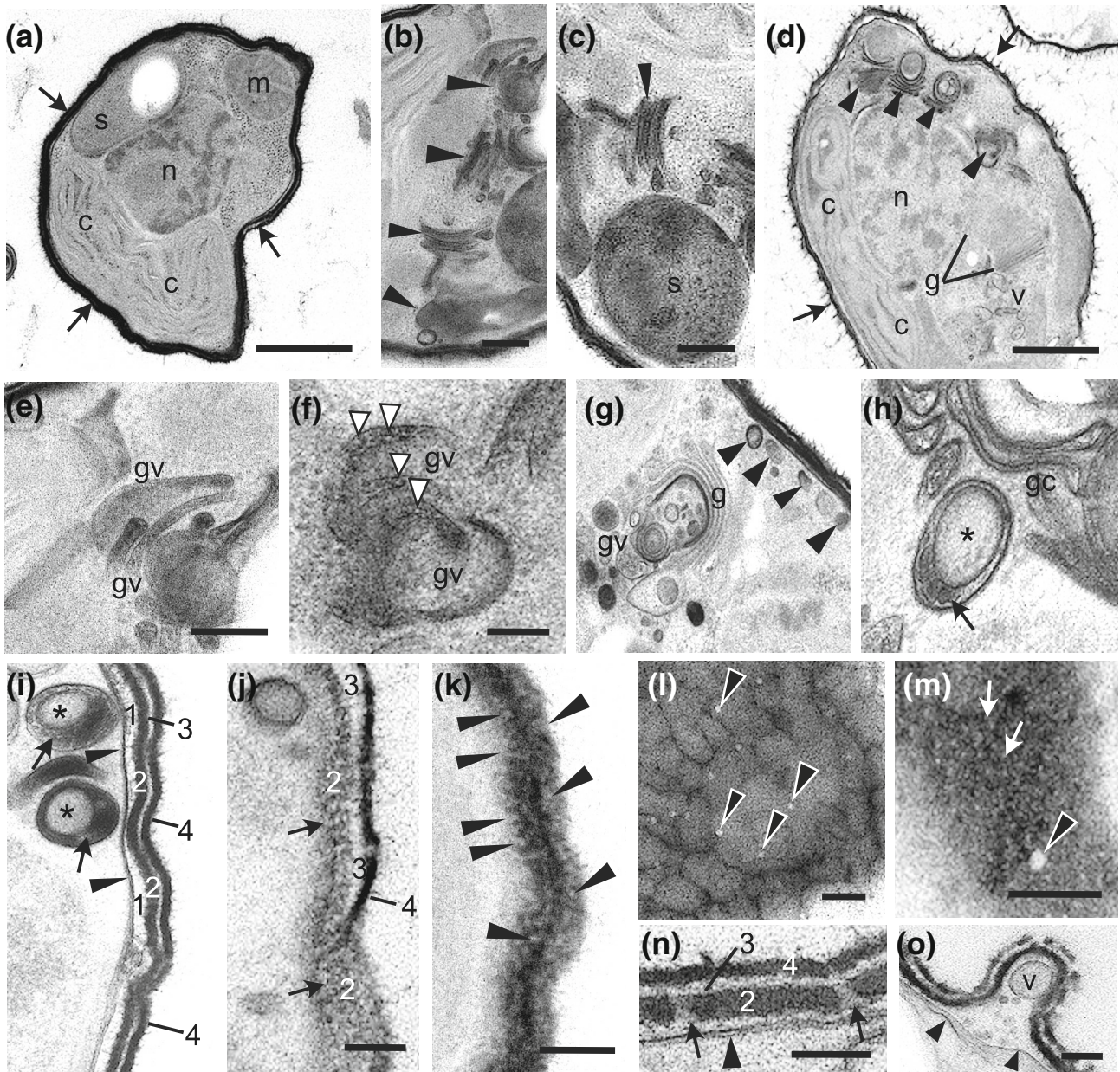


FIG. 7. Fine structure *Chromopallida australis* gen. et sp. nov. (a) Section near the middle of a cell showed a nucleus (n), mitochondrion (m), a storage structure (s) and the chloroplast (c). The multilayered PT (arrows) was seen as a single, electron dense layer (c. 120 nm thick) at this magnification. (b) Multiple Golgi stacks (arrowheads) accumulated adjacent to the nucleus (beneath the plane of this section) with cisternae containing electron dense contents. (c) A storage vesicle (s) of unusual morphology was observed towards the center of the cell near a Golgi stack (arrowhead). (d) Golgi stacks (arrowheads) closely spaced and adjacent the nucleus (n) with 5–7 cisternae, contents electron dense. A second type of Golgi stack (g) had a different morphology, was larger with 15–20 cisternae without electron dense contents. Vesicles (v) at the distal, mature Golgi face are multilayered without dense contents. The outer layer of the PT often had spiked extensions of variable length (arrows). (e, f) Golgi vesicles (gv) with electron dense contents that have a porous morphology (arrowheads). (g) Large Golgi stack (g), the distal faces observed to have multilayered vesicles (gv). Vesicles (arrowheads) lie adjacent to the PM. (h) Golgi cisternae (gc) at the distal mature face and a multilayered vesicle (asterisk). (i) The PT had four extracellular layers (1, 2, 3, 4), adjacent the PM (arrowheads) layers 2 and 4 were electron dense while layers 1 and 3 were narrow and lightly stained. Multilayered vesicles (asterisk) near the PM contain electron dense layers (arrows) the same thickness as the PT. (j) Glancing section through the PT showed the porous nature of layer 2. Tiny pores c. 10–12 nm in diameter were observed (arrows). (k) Glancing section through the PT showing pores in both layers 2 and 4 (arrowheads). (l, m) Tangential sections through the PT showed scattered macropores (18–20 nm, black arrowheads), while the tiny pores are more equally spaced (m, white arrows). (n) Cross-section of the PT showed all 4 layers out from the PM (arrowhead), layers 2 and 4 electron dense. Two macropores (arrows) in cross-section appeared to penetrate layer 2 only. (o) An extracellular vesicle (v) was located in the space between the PM (arrowheads) and layer 2 of the PT. Scale bars = 1.0 μ m (a, d), 200 nm (b, c, e, g, h), 100 nm (f, i–n), 50 nm (o).

rounding up (Fig. 6, m–o). Cells continued to divide, producing colonies of sarcinoid packets typically containing 4, 8 or 16 closely packed cells surrounded by 1–3 gelatinous sheaths that were best observed when stained with toluidine blue (Fig. 6, n and o). Clusters of colonies were embedded in large quantities of mucilage that adheres to the substratum (e.g., sand; Fig. 6o). Eventually, the colonies disperse into single cells (Fig. 6g) prior to undergoing another round of divisions. Cells were surrounded by a PT with distinct pores when viewed with transmission electron microscopy (see below). Cell wall and mucilage layers can be stained (Fig. 6, j, m–o) but appeared to disperse when the colonies disassociated prior to the subsequent division cycle. Vegetative colonial reproduction was by cluster fragmentation and we never observed zoospores in any stage of the vegetative cycle in cultures.

Fine structure. The HPF fixation of this species was good and most cytoplasmic organelles and structures were observed, including the PM and PT (Fig. 8, a–o). Cell wall and mucilage layers were less electron dense but still observed. Cells were uninucleate with the chloroplast lobes dominating the cell cytoplasm (Fig. 8, a and d) and stalked pyrenoids surrounded by a closely associated, flattened out cisterna (Fig. 8m). Large Golgi stacks were observed, the forming face abutting the nucleus and a range of vesicles types associated with the mature, distal Golgi face (Fig. 8, b and c). Cells were covered by an undulating PT consisting of two layers, a mildly fibrous #1 layer that was sandwiched between the PM and layer #2, an electron dense perforated layer that was uniform in thickness (25–30 nm). Layer #1 had no apparent substructure and varied in thickness, accounting for the overall undulations (Fig. 8, d–g). Level #2 was observed in glancing sections to contain a high concentration of pores embedded in an electron dense matrix (Fig. 8, f–i), the pores being uniform in size (20–22 nm in diameter) and appearing to contain material (arrowheads, Fig. 8i). Cytoplasmic vesicles were concentrated near the Golgi stacks and adjacent to the PM, many appearing long and tubular (Fig. 8, c and k) or multilayered with varying contents (Fig. 8, b, c, e, j, and k). Vesicles were seen between the plasma membrane and the level #2 within a pocket of layer #1 (Fig. 8l), but not fused with the PM, while an adjacent image in the same figure showed a similar pocket but devoid of a vesicles or other discernible material.

The PT across Pelagophyceae. In order to ascertain whether a PT is the first morphological feature to define the Pelagophyceae, as we have hypothesized (Wetherbee et al. 2021), the following genera in diverse lineages of the class were prepared by HPF in order to ascertain and characterize the presence of a PT; *Chrysoreinhardia*, *Andersenina*, *Sungminbooa* and *Sargassococcus*. As with the other genera of

Pelagophytes we have investigated, the quality of the HPF fixation varied for cytoplasmic organelles and structures, although the PM, PT and most cell wall/mucilage layers were well preserved.

Chrysoreinhardia giraudii: As described by previous workers (e.g., Han et al. 2018), the Australian strain of this species alternated between benthic packets of golden brown cells (Fig. 9, a and c) and a heterokont flagellate (Fig. 9, d and e). Sarcinoid packets consisting of 4, 8, 16 or more cells were surrounded by mother cell walls, grandmother cell walls, etc (Fig. 9, a and b) and secreted large amounts of adhesive mucilage. Cells on the surface of cell clusters routinely divided to produce imbricated daughter cells (Fig. 9c) that transformed into zoospores within the mother cell wall (Fig. 9d). The heterokont flagella formed within the mother cell wall before the zoospores emerged as the motile generation (Fig. 9, d and e).

The HPF fix was particularly good for this species and revealed several interesting, novel features (Figs. 9, f–n and 10, a–l). Cells were uninucleate and lobes of the chloroplast(s) dominated the cytoplasm along with large storage vesicles (chrysolaminarin?; Fig. 9, f and g). Cells were bound by a PT tightly appressed to the PM, and together they could sharply undulate over the cell surface (Fig. 9, f–i, m, n), particularly at a cleavage furrow where large invaginations were observed in light and electron microscopy (Fig. 9, c and g). During early development at the cell cleavage, the PM the PT layer #2 are almost indistinguishable (Fig. 9j). The PM is 12 nm in width while the outer surface is more electron dense (Fig. 9k). A thin fibrous layer #1 (12–18 nm in width) became visible at higher magnification (Fig. 9, k and m) and is sandwiched between the PM and the single perforated layer #2 (25–35 nm in width) that is porous with small interconnecting pores (c. 10 nm) seen in glancing sections (Fig. 9, l–n). A relatively transparent, fibrous layer of varying thickness (asterisk, Figs. 9, i, m and 10, a, c, f, g, i, l) was observed between the PT and a more electron dense cell wall (Figs. 9, f, h, m and 10, a, c, g, l), the latter expanding following division to surround daughter cells (i.e., a mother cell wall; Fig. 9g).

Large Golgi stacks were observed (Fig. 10, a and b), the forming faces abutted the nucleus while the distal face was associated with an assortment of vesicles, many multilayered, that appeared as vesicles within vesicles (Fig. 10, c and d). Vesicles with different morphology appeared to be in stages of fusing to form the multilayered vesicles (Fig. 10d) and the resulting vesicles were observed in patches in the cytoplasm and between the Golgi and PM (bracket, Fig. 10, a–e). Vesicles with lightly fibrous contents and surrounded by a single membrane (i.e., not multilayered) were observed tightly appressed to the PM (v1, Fig. 10, f and g), while other vesicles of similar morphology were

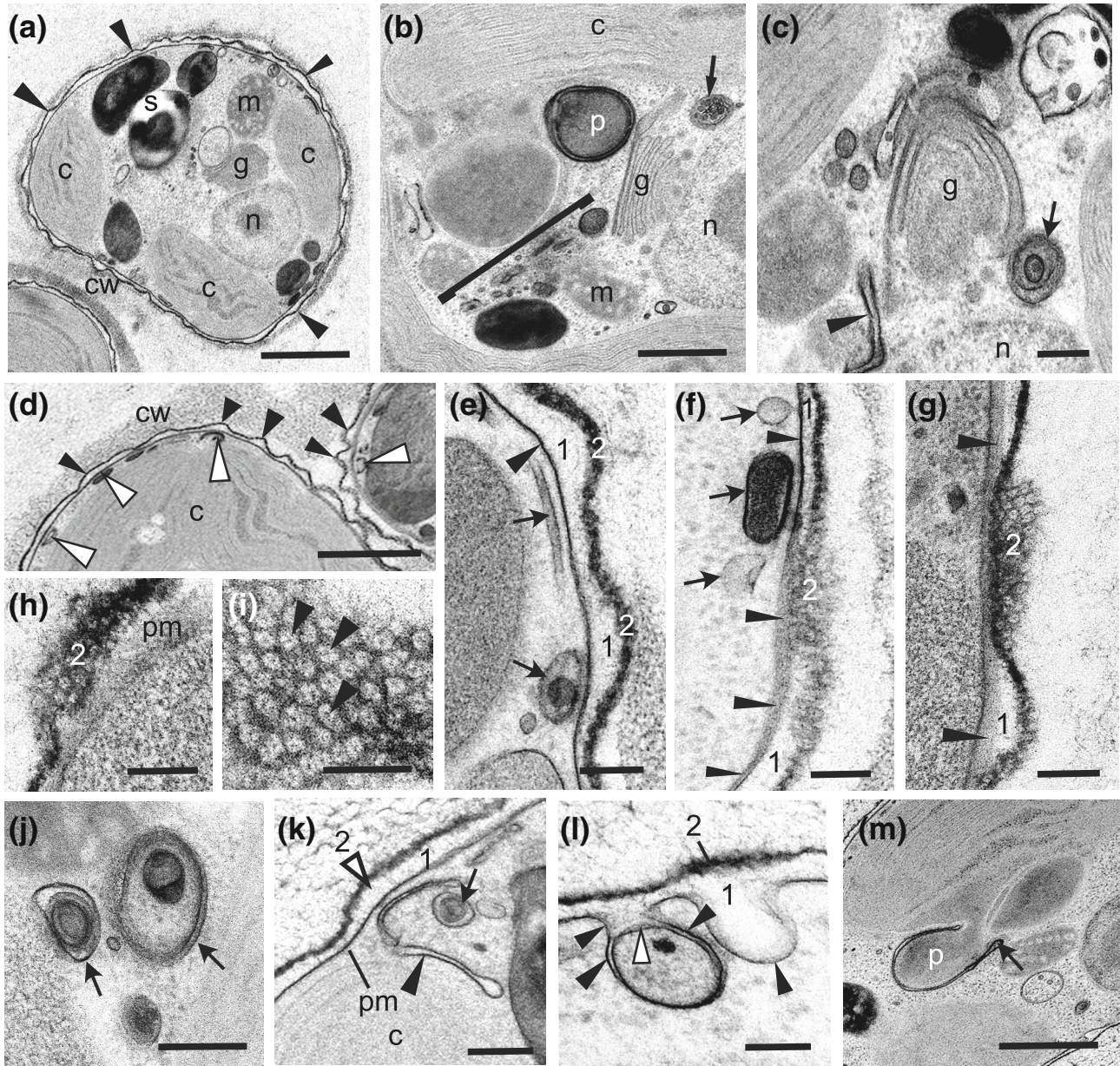


FIG. 8. Fine structure of *Pituiglomerulus capricornicus* gen. et sp. nov. (a) Section through a cell that showed the chloroplast(s) (c), nucleus (n), Golgi stack (g), mitochondrion (m) and storage vesicle (s). The PT (arrowheads) surrounded the cell. (b) Low magnification image showed a glancing section through the stalked pyrenoid (p), a large Golgi stack (g) with the forming face adjacent to the nucleus (n) and the distal face near a range of vesicles of various morphology (bar), some multilayered (arrow). (c) Golgi stack (g) with long thin vesicles (arrowhead) and multilayered vesicles (arrow) observed in the adjacent cytoplasm. (d) The PT (black arrowheads) undulated over the cell surface while vesicles aligned under the PM (white arrowheads). (e–g) Perforated layer #2 of the PT was uniform in thickness while layer #1 varied considerably. Vesicles (arrows) that differed in morphology accumulated beneath the PM (arrowheads), which was observed to have a belt like appearance in glancing sections. Packed pores in layer #2 were seen in glancing section. (h, i) High magnification of the pores in layer #2 that appeared to have contents (arrowheads). (j) Multilayered vesicles (arrows) were seen throughout the cytoplasm. (k) Tubular (arrowhead) and multilayered (arrow) vesicles accumulated near and PM and PT layers 1 and 2. (l) Vesicle surrounded by the PM (black arrowheads) and embedded in layer #1 of the PT. Note the vesicle membrane was not observed to fuse with the PM. An adjacent pocket of layer #1 is empty. (m). Stalked pyrenoid (p) surrounded by a flattened cisterna (arrow). Scale bars = 2.0 μm (a), 1.0 μm (b, d, m), 0.5 μm (c), 100 nm (e–i, k, l), 0.5 μm (h), 200 nm (j).

extracellular, positioned between the PM and perforated layer #2 within layer #1 of the PT (v2, Fig. 10, f, g and h). Similar extracellular vesicles were observed associated with large invaginations of the

PM/PT, once again positioned extracellularly outside the PM and below layer 2 of the PT (Fig. 10, i and j). These vesicles were never observed to fuse with the PM, but vesicles of similar size and position

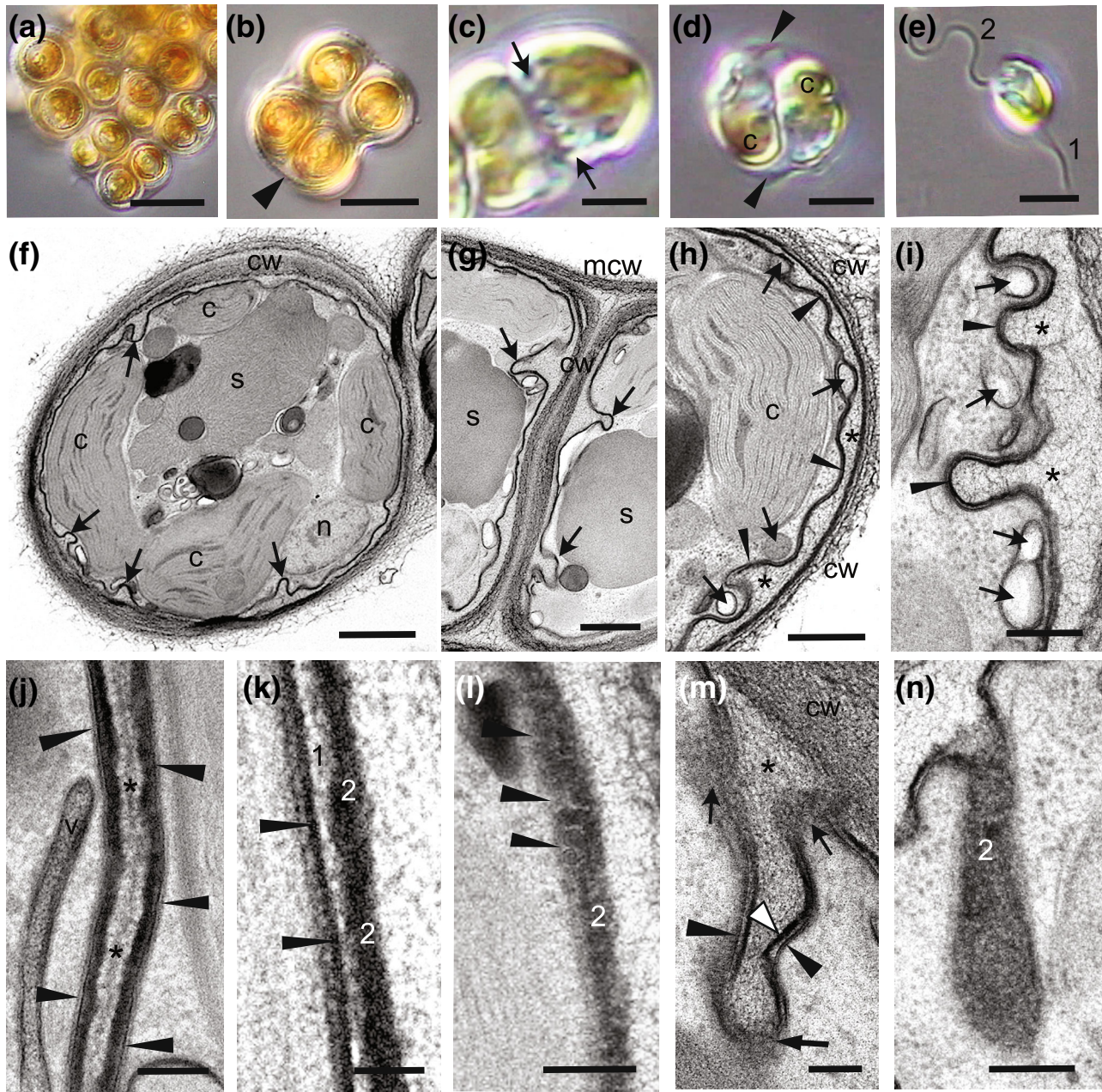


FIG. 9. Light microscopy and fine structure of *Chrysoeinhardii giraudii*. (a) Clusters of cells in sarcinoid packets adhered together. (b) Packet of four cells surrounded by mother cell walls and a grandmother cell wall (arrowhead). (c) Recently divided cell showed the undulating cleavage furrow of one of the daughter cells (arrows). (d) Recently divided cell within the mother cell wall, produced two zoospores in opposite orientation with chloroplasts (c) at the future apex of cells. Flagella were forming (arrowheads). (e) Zoospore had heterokont flagella, the forward beating immature flagellum 2 and the trailing mature flagellum 1. (f) Section through the center of a cell showed the extensive chloroplast coverage (c) plus a large storage vesicle (s), the nucleus (n) and cell wall (cw). The PM and adjacent PT invaginated into the cell at several points (arrows). (g) Cleavage furrow (asterisk) formed between two daughter cells, each with a cell wall (cw) and surrounded by a mother cell wall (mcw). Invaginations of the PM and associated PT (arrows) were extensive in this region. Storage vesicles (s) were prominent. (h, i) The unusual undulating PM/PT (arrowheads) was observed with vesicles aligned beneath (arrows). A mucilage layer (asterisk) was observed between the PT and cell wall and was particularly obvious at the sites of invagination. (j) Cleavage furrow (asterisk) between two recently divided cells. The PM (arrowheads) is indistinguishable from the single perforated layer 2 of the PT. (k) As daughter cells matured, a thin layer 1 of the PT was distinguished, sandwiched between layer 2 and the PM, which has a thick, denser, inner surface (arrowheads). (l) Glancing section through the perforated layer 2 showed an electron dense, grainy porous structure (arrowheads). (m) Deep invagination of the PM (black arrowheads) and PT (white arrowhead) into the cell had the look of train tracks. Several regions of the PT were in glancing section where the porous structure was observed (arrows). A mucilage layer (asterisk) separated the PT from the cell wall. (n) Glancing section through perforated layer 2 of the PT at a large invagination showed its grainy, porous structure. Scale bars = 10 μm (a, b), 5 μm (c–e), 1.0 μm (f, g), 0.5 μm (h), 250 nm (i, n), 100 nm (j, l, m), 30 nm (k). [Color figure can be viewed at wileyonlinelibrary.com]

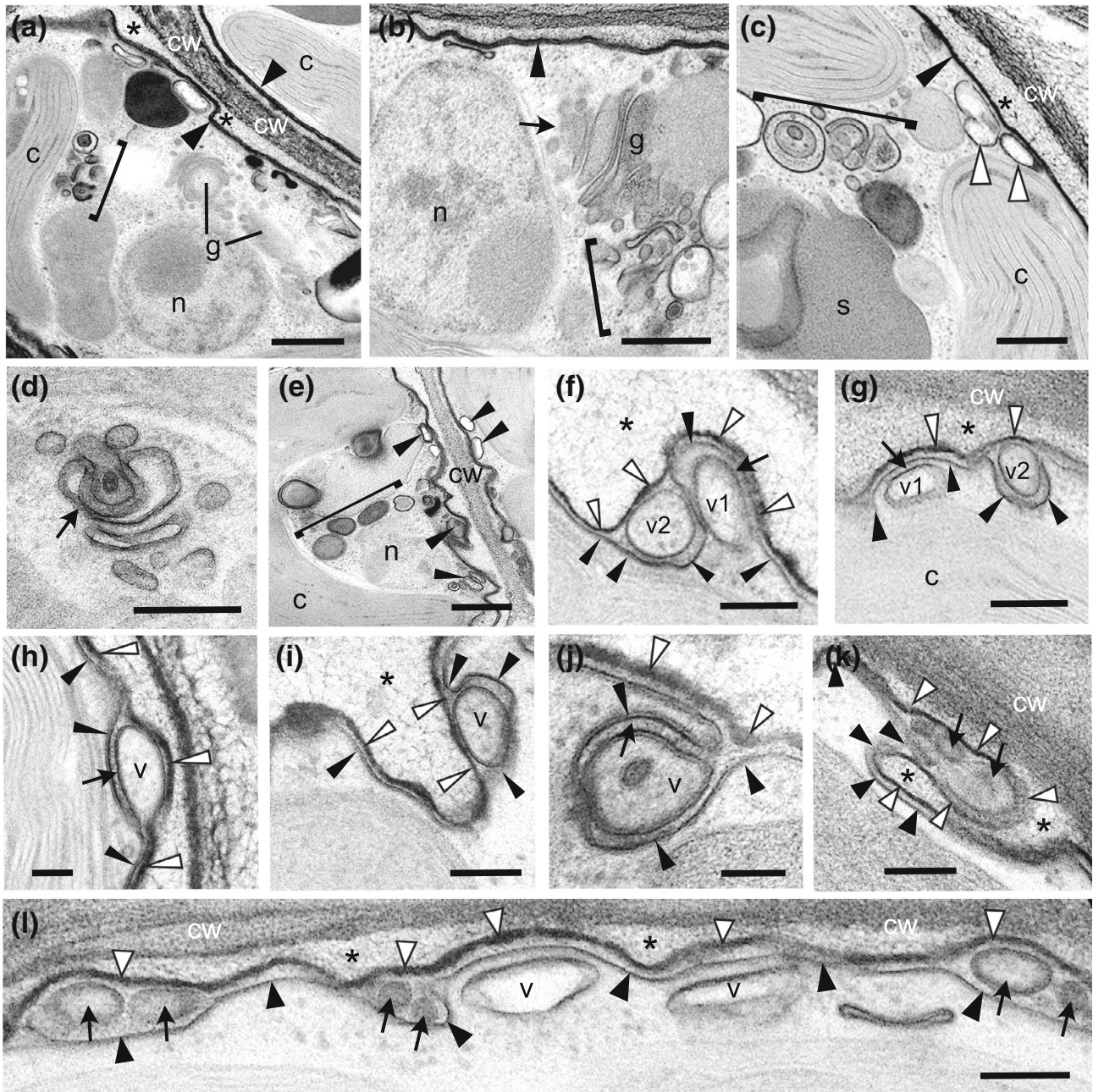


FIG. 10. Fine structure of *Chrysoeinhardii giraudii*. (a) Section showed the electron dense PM-PT of two cells (arrowheads) separated by mucilage layers (asterisk) and cell wall (cw). Golgi stacks (g) positioned near the nucleus (n) with an accumulation of diverse vesicles located in the cytoplasm (bar) and adjacent the PM. (b) Forming face (arrow) of the Golgi (g) adjacent the nucleus (n), and the vesicles of various size and morphology were observed at the distal face (bar). (c) Multilayered vesicles accumulated in the cytoplasm (bar) while vesicles with a fibrous content (white arrowheads) accumulated beneath the PM-PT (black arrowhead). A mucilage layer (asterisk) was sandwiched between the PT and cell wall (cw). (d) Multilayered vesicles appeared to originate from the fusion of vesicles with different contents (arrow). (e) Junction of two cells separated by a cell wall (cw). Vesicles (bar) dominate the cytoplasm and adjacent the PM (arrowheads). (f, g) Two stages in the interaction between the PM (black arrowheads) and PT (white arrowheads) and adjacent vesicles were observed. Vesicles closely align with the PM (arrows, v1) but were never observed to fuse. The second stage showed vesicles to be extracellular (v2), embedded between the PM, which had formed around the vesicles, and perforated layer 2 of the PT. (h-j) Extracellular vesicles (v) embedded between the PM (black arrowheads) and perforated layer 2 of the PT (white arrowheads). Note the close connection between the vesicle membrane with the PM (arrows) in h and j. (k, l) Extracellular vesicles were observed in various stages of what appeared to be disintegration (arrows), the vesicles observed within layer 1 of the PT, between the PM (black arrowheads) and perforated layer 2 of the PT (white arrowheads). Other cytoplasmic vesicles (v) are positioned adjacent to the PM. Scale bars = 0.5 μm (a-e), 200 nm (f, g, j), 100 nm (h, i, k, l).

were observed in stages of apparent disintegration, many with indistinct membranes (Fig. 10, k and l).

Sargassococcus: This genus was recently described in Han et al. (2018) without the benefit of TEM. Fixation of this genus with HPF was successful (Fig. 11, a–k). The PT consisted of two layers, a thin, perforated layer #2 (12–14 nm) that was only marginally thicker than the PM and separated from it by a lightly stained layer #1 (20–24 nm) that

was traversed by thin fibers perpendicularly spaced between layer #2 and the PM and gave the overall appearance of train tracks (Fig. 11a). Layer #2 was densely packed with pores 18–22 nm in diameter (Fig. 11c) appearing lumpy in cross-section (Fig. 11a). Numerous, large “peripheral vesicles” often pressed against the PM, were lightly stained and contained some fibrous material (Fig. 11, b, d, h, i and k). Multilayered vesicles, or vesicles within

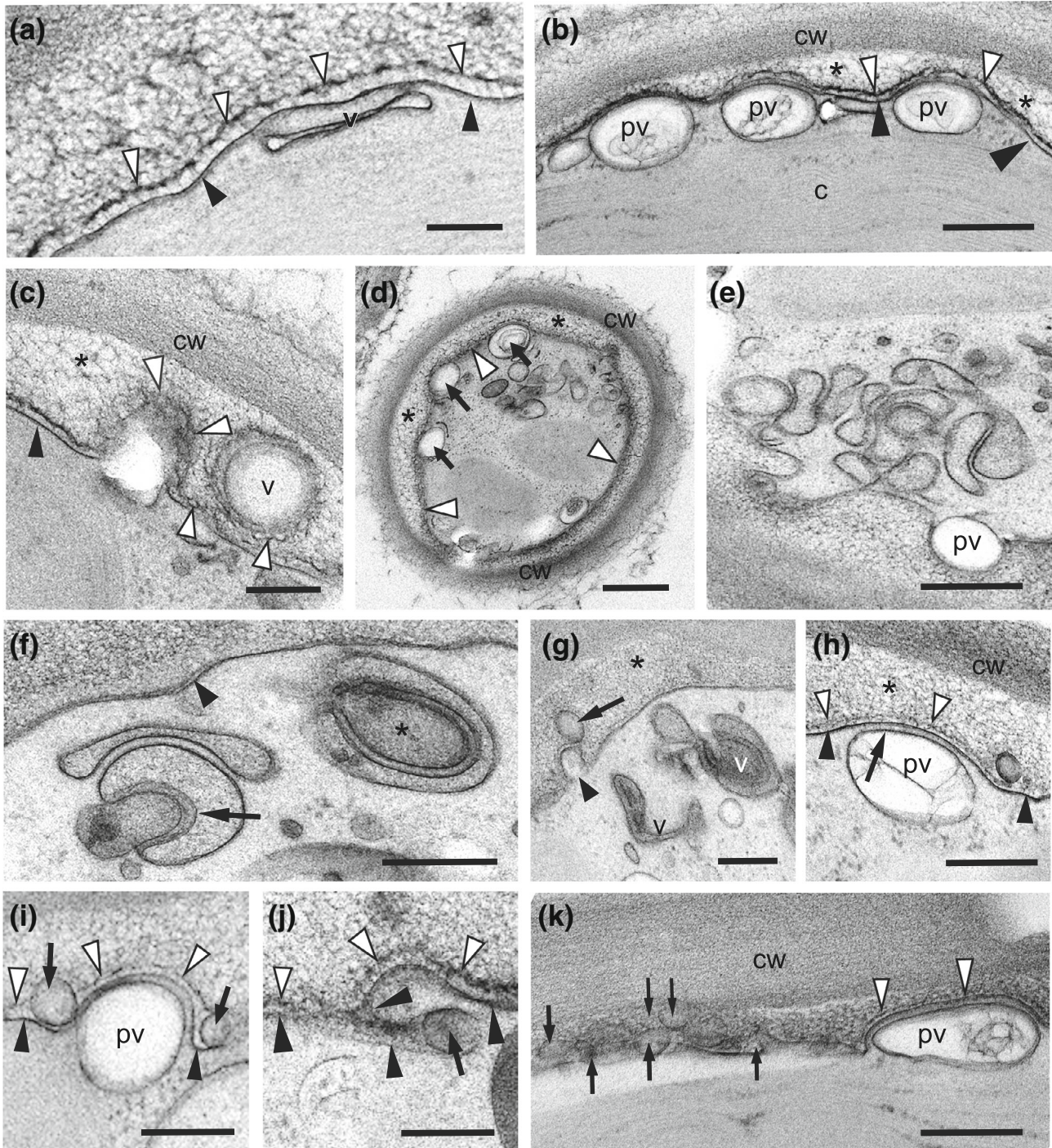


FIG. 11. Fine structure of *Sargassococcus* sp. (a–j) The HPF fix of this species was very good for the PM-PT and associated vesicles. (a) Layer 2 of the PT (white arrowheads) was very thin (12–15 nm), only marginally thicker than the PM (black arrowheads, 10–12 nm), while layer 1 was fairly uniform in thickness (25–30 nm) with fibers running perpendicular to the PM and layer 2, the PM-PT together appeared like train tracks. (b–j) Vesicles differed in morphology throughout the cytoplasm and often appeared adjacent the PM, though no vesicles were ever observed to be fusing with the PM. (b) Peripheral vesicles (p) were common in this species and tightly appressed to the PM (black arrowheads) and contained lightly stained fibrous material (see also h and j). The PT (white arrowheads) was separated from the cell wall (cw) by a slightly stained mucilage layer (asterisk) of various thickness. (c) Pores of the PT were seen in glancing section (white arrowheads) of two vesicles protruding out from the cell surface, both still connected to the cell surface in other sections. Vesicles appeared to eventually become extracellular and were located in layer 1 of the PT but surrounded by layer 2. (d) Glancing section through the tip of a small cell that showed peripheral vesicles (arrows) and the PM-PT (white arrowheads) surrounded by a mucilage layer (asterisk) and the cell wall (cw). (e) Collection of vesicles near the undulated cell surface plus a peripheral vesicle (pv). (f) Multilayered vesicles (asterisk) appeared to arise from the fusion of vesicles with differing contents (arrow). PM-PT (arrowhead). (g) Multilayered vesicles (v) near the PM, but only vesicles surrounded by a single membrane with a uniform content were seen to protrude from the cell surface (arrowheads) and become extracellular, located within layer 1 of the PT. Perforated layer 2 always separates the vesicles from the mucilage layer (asterisk). Vesicles were observed to be separated from the cells (e.g., arrow) but serial sections showed they were connected. (h) Peripheral vesicle (pv) was adjacent the PM – PT (black and white arrowheads) train tracks with a uniform space between the pv membrane and the PM. (i) Peripheral vesicle (pv) located beneath the PM (black arrowheads) and PT (white arrowheads). Two adjacent small vesicles (arrows) have relocated between the PM and layer 2 of the PT and appeared to be in a state of disintegration. (j) PT perforated layer 2 (white arrowheads) and PM (black arrowheads) were observed to be separated as a vesicle (arrow) was enclosed within layer 1 of the PT and appeared to be in a state of disintegration. (k) The membrane of a peripheral vesicle is tightly appressed to the PM – PT train tracks (white arrowheads), while multiple other vesicles were in states of apparent disintegration (arrows). The extremely thin PT could not be followed due to the excessive activity at this location on the cell surface. Scale bars = 100 nm (a), 250 nm (b), 200 nm (c, f–k), 0.5 μm (d, e).

vesicles, were observed throughout the cytoplasm and appeared to result from the fusion of vesicles that possessed different contents (Fig. 11, f and g). Vesicles with varying contents are observed near or adjacent to the PM-PT, occasionally appearing embedded in layer #1 between the PM and the perforated Layer #2 in evaginations (Fig. 11, c, g, i–k). Vesicle contents often appeared to be in a process of disintegration within the evaginations of the PT resulting in a very irregular PM-PT surface (Fig. 11, g and i–k). The thin perforated layer #2 was difficult to discern in regions of apparent active secretion (e.g., Fig. 11, g, i–k), but appeared to surround the disintegrating vesicles (Fig. 11, c and g).

Anderseniania: The only filamentous member of this class (Wetherbee et al. 2015), the HPF fix was good for the PM-PT complex and adequate for some cytoplasmic organelles and structures (Fig. 12, a–i). The PT consisted of only two layers, the standard fibrous layer #1 (generally 20–25 nm thick) that was sandwiched between the PM and perforated layer #2 (25–30 nm thick) that was porous (grainy) with small interconnected pores 10–12 nm in diameter (Fig. 12, b–e). Golgi stacks were observed with the forming face adjacent to the nucleus and vesicles of various morphology observed near the distal Golgi face and in the cytoplasm (Fig. 12, f and g). Extracellular vesicles were observed embedded within PT layer #1 between the PM and perforated layer #2, often appearing to be in a state of disintegration (Fig. 12, h and i).

Sungminbooa: This genus was recently described in Han et al. (2018) without the benefit of TEM. Our HPF fix was excellent for the PM and PT but cytoplasmic organelles and structures were not generally well preserved (Fig. 12, f–n). The perforated layer #2 appeared directly adjacent the PM (Fig. 12,

j–l) and was a thick, densely porous layer (45–55 nm thick) with packed, small pores (14–18 nm in diameter; Fig. 12, j–l) best seen in glancing section (Fig. 12m). The space between the PM and PT (level #1 in other pelagophytes) was typically very narrow and hard to see in cross-section (Fig. 12, k and l), but observed in glancing sections, which enhanced its presence (e.g., Fig. 12m). Golgi stacks and vesicles of various morphology, including multilayered vesicles (v), were observed, particularly orientated next to the PM (Fig. 12, l and n).

Evolution of the PT: We attempted to show the distribution of some PT-related traits on a phylogenetic tree of the pelagophytes trimmed down to those taxa for which trait information is available (Fig. 13). Thecal thickness varied substantially, with particularly those in the *Chromopallida-Ankylochrysis-Wyeophycus* clade being thicker than those of other lineages. The Sarcinochrysidales all have 2 PT layers, whereas in Pelagomonadales the ancestral state is inferred to be 4 layers, with the *Pelagomonas* PT reduced to a single layer and *Wyeophycus* having added a fifth layer. The state at the base of the phylogeny could not be inferred with confidence, with nearly equal probabilities for 2 or 4 layers.

DISCUSSION

Phylogeny and habit. Our phylogenetic results based on five chloroplast genes and nuclear 18S rDNA gene sequences show that *Wyeophycus*, *Chromopallida* and *Pituiglomerulus* all form relatively deep-branching lineages of pelagophytes that, in combination with their morphological features, support their recognition as new species and genera. While *W. julieharrissiae* and *C. australis* are clearly related to *Ankylochrysis*, the inferred sister relationship

between *P. capricornicus* and *Chrysoctysis fragilis* in the Chrysoctyidae is less well-supported. *Wyeophycus julieharrissiae* and *P. capricornicus* are both benthic and sand-dwelling but differ significantly in morphology and their method of adhesion and dispersal in a dynamic tide pool habitat. *Chromopallida australis* on the other hand is a flagellate for which we have not observed any benthic stage.

Wyeophycus julieharrissiae has a novel approach for the dispersal of benthic cells in sand not seen in other pelagophytes or heterokonts that we are aware of. Cells are strongly adhered to the substratum yet able to quickly detach and become motile if conditions require it, possessing short flagella that are only activated on release, producing short strokes that result in cells fluttering and spinning in their

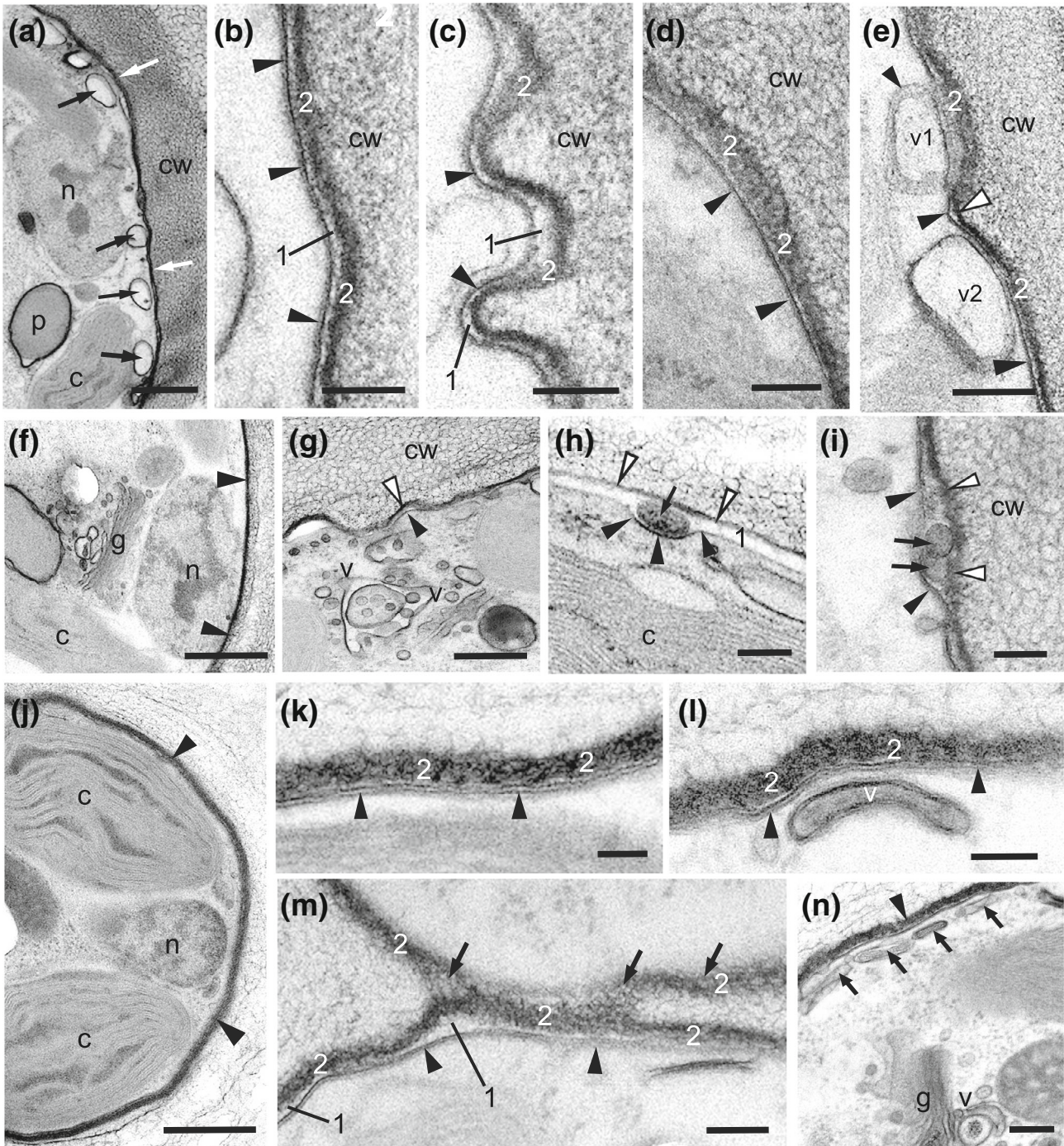


FIG. 12. Fine structure of *Andersenella nodulosa* (a–i) and *Sungminbooa* sp. (j–n). (a) Edge of a cell in a filament of *A. nodulosa* showed the combined PM and PT at this magnification (white arrows), cell wall (cw), nucleus (n), chloroplast (c) and glancing section of a stalked pyrenoid (p). Vesicles with lightly stained contents were adjacent to the PM (black arrows). (b, c) Cross-sections of the PM (black arrowheads) and PT, comprised of a lightly stained layer 1 of varying thickness plus a densely stained, perforated layer 2. (d) Glancing section through layer 2 showed a grainy, porous structure. (e) Two vesicles were observed adjacent to the PM, one vesicle in glancing section (v1) suggested it was extracellular and enclosed between the PM and perforated layer 2. An adjacent vesicle (v2) was closely abutting the PM but not extracellular. (f) A large Golgi is observed with the forming face adjacent the nucleus (n) near the PM-PT (arrowheads). (g) Products of the Golgi were often multilayered, or vesicles within vesicles (v). (h, i) Vesicles (arrows) were never observed to fuse with the PM (black arrowheads), but were observed within layer 1 of the PT, sandwiched between the PM and perforated layer 2 (white arrowheads) of the PT, and appeared in a stage of disintegration (arrows). (j) Section of a *Sungminbooa* cell showed and generally good HPF fixation, including the chloroplast (c), nucleus (n) and the combined PM-PT (arrowheads) seen together at this magnification. (k, l) The PT has only a very thin layer 1, which was often not visible, and a thick, electron dense, perforated layer 2, which abutted the PM (arrowheads). Vesicles (v) often appeared adjacent to the PM. (m) Layer 2 was seen in glancing section outside of the PM (arrowheads) at a cleavage furrow between two cells. Layer 1 and the porous structure of layer 2 (pores 12–15 nm in diameter) were observed (e.g., arrows). (n) Large Golgi (g) and associated vesicles (v) were observed as well as vesicles (arrows) lined up beneath the PM-PT (arrowhead). Scale bars = 0.5 μm (a, f, g, j), 100 nm (b–d, h, i, m), 200 nm (e, n), 50 nm (k, l).

search for resettlement. Retaining largely stagnant flagella in the benthic stage is a novel adaptation for the instant dispersal of benthic cells and does not require cells to first recognize the need to relocate and then either generate new flagella or wait until zoospores are formed following division. The unusual fluttering motility seemingly results from the short anterior flagellum's inability to produce a sinusoidal wave that would pull the cells behind it, which is in sharp contrast to the normal heterokont condition in other pelagophytes with a long anterior flagellum.

In *Chromopallida australis* the flagellates do not alternate with a benthic stage but are always planktonic. Cells have the appearance of being colorless, as even a pellet of cells lacks much color and flasks of concentrated cells appear as media alone. The slender, tubular chloroplast has no unusual fine structural features, so chloroplast size alone probably accounts for the cells almost colorless appearance, particularly compared to sister genera *Wyeophycus* and *Ankylochrysis* (Honda and Inouye 1995), as well as most pelagophytes where cells are heavily pigmented and chloroplasts often dominate the cytoplasm (e.g., Han et al. 2018).

Pituiglomerulus capricornicus is comprised of sarcinoid colonies in cubic packets, a morphology that is common throughout the Sarcinochrysidales, particularly in the benthic species of *Chrysoreinhardtia*, *Glomerochrysis*, *Sarcinochrysis*, *Sargassococcus* and *Sungminbooa* (for review, see Han et al. 2018, Wetherbee et al. 2021), and the relationships between these genera are only known by DNA sequences. With this type of benthic habit, colonies reach a certain size before fragmenting into smaller colonies or cell packets for dispersal, a mechanism that would be enhanced when clusters are subjected to the movement of tide pool sand. Some species occasionally produce heterokont zoospores to further extend their distribution, though we never observed zoospores in *P. capricornicus*.

Ultrastructure of the pelagophyte PT. Our fine structural studies on the pelagophytes have featured

fixation by HPF (Wetherbee et al. 2021), the quality of the preservation varying between species for cytoplasmic features (e.g., organelles) but has been consistently good for the preservation of the plasma membrane, PT and most associated extracellular wall and mucilaginous layers. The Golgi and vesicles of the endomembrane were also generally well preserved and appeared involved in the production and secretion of PT rafts as well as materials for the formation of extracellular walls and mucilage layers exterior to the PT.

Our observations described in this paper include three newly described genera plus four other representative genera from major lineages of the Sarcinochrysidales that have not been previously examined with HPF preparation. Results confirm our initial hypothesis that a PT is the first morphological feature to define the Pelagophyceae. Our initial characterization of the PT was based on three genera from the Sarcinochrysidales (*Gazia*, *Glomerochrysis* and *Aureoumbra*), and we defined the PT as “a dense outer covering or sheath penetrated by distinctive pores”. We now modify and extend that definition as follows: a multilayered cell covering that encases entire cells except where flagella emerge in flagellates and zoospores, possessing one or two electron dense, perforated layers interspersed with less dense fibrillar layers that all together form the perforated theca”. Two distinctive types of PT are reported here, a 4 or 5 layered PT found thus far only in genera of the Pelagomonadales, while a thinner, two layered PT is restricted to genera of the Sarcinochrysidales (summarized in Table 1).

In a commentary highlighting our recent paper (Wetherbee et al. 2021), Moestrup (2021) took exception to the term “theca” being used to describe the cell covering of pelagophytes and proposed “periplast” instead. Periplast is a term that has been used almost exclusively to define the complex cell covering of cryptomonad flagellates, comprised of both inner and surface periplast components that sandwich the plasma membrane over most of the cell surface, but is absent from a vestibulum where

flagella emerge and secretions occur. Periplast components are also absent where ejectisomes (projectile organelles) systematically occur at several locations at the cell surface. Therefore, the cryptomonad periplast differs significantly from the pelagophyte cell covering, where the extracellular PT surrounds entire cells except where flagella emerge in flagellates and zoospores. “Theca” has become a well-known generic term used across many algal divisions to refer to cell coverings, or components of cell coverings. Historically, theca was first used to describe the cell covering of the pelagophyte *Ankylochrysis lutea* (van der Veer 1970), a species originally assigned to the chrysophytes before being transferred to the Pelagophyceae (reviewed in Han et al. 2018). Later the term theca was used in the description of *Pelagomonas* and the establishment of the class Pelagophyceae (Andersen et al. 1993). In the few published reports using ultrastructure to describe pelagophytes, the cell covering has never been referred to as a periplast. Moestrup (2021) also suggested workers might invent new terms for all the algal taxa where theca has been used, as recommended in a review by Preisig et al. (1994). Since that time this recommendation has not been generally acted on, including by Moestrup who co-authored the review. In our opinion, a switch to using periplast over PT has little merit.

PT Layers 1 and 2 are observed in all species observed to date. Layer 1 abuts the PM and is only slightly stained but often has equally spaced fibers

that run perpendicular between the PM and layer 2 that is always electron dense. If layer 2 is thin (10–14 nm), the PT has the appearance of train tracks as seen in this paper (e.g., see Figs. 9, h–m; 11a; 12, a and b) and the three genera described in Wetherbee et al. (2021). In *Pituiglomerulus capricornicus* layer 1 undulates over the surface and varies considerably in thickness (e.g., Fig. 8, a and e–g), but this is unusual. Layer 2 always follows the contour of layer 1 and is perforated with either micropores (10–14 nm in diameter) or macropores (18–22 nm in diameter), or occasionally both pore sizes (see *Gazia australica*, Wetherbee et al. 2021).

In species with 4 or 5 total layers from the Pelagomonadales, including *Wyeophycus julieharrissiae* and *Chromopallida australis* described here, layer 3 is like layer 1, with or without perpendicular columns that may define complex pores in a honeycomb configuration (e.g., Fig. 3, e–g). Layer 4, like layer 2, is always electron dense and perforated with micropores and occasionally macropores as well and may produce protrusions on the surface. In *W. julieharrissiae* a layer 5 develops on the cell surface, is not as electron dense as layer 4 and can produce fibrillar protrusions. In the related genus *Ankylochrysis lutea* a bilayered cell covering was described by Honda and Inouye (1995), but using the terminology described here there are four layers; the two electron dense layers (layers 2 and 4) were described, but the two lightly stained layers (i.e., layers 1 and 3) were not included in the authors description of the cell covering (see figs. 16 and 17, in Honda and Inouye 1995). If you look closely at layer 2 in figure 16 of the same paper, you can see pores that would be obvious at higher magnification. By the authors admission, the preservation of the cell covering was a problem with the fixations utilized at that time.

A 4-layered cell covering has also been observed in two other genera of the Pelagomonadales, *Pelagococcus* and *Aureococcus*. *Pelagococcus subviridis* was described as having a covering of three layers (Vesk and Jeffrey 1987), but we recognize four layers by our terminology in their figures 6–8. Although the electron dense layers were not observed to be perforated, pores are obvious in layer 2 (Figs. 7, 8 and 12). In figures 6 and 7, also in Vesk and Jeffrey (1987), layer 3 appears to have perpendicular fibrils that could possibly reveal the honeycomb structure seen in *Wyeophycus julieharrissiae* if fixed by HPF. In a single, low magnification TEM image of *Aureococcus anophagefferens* (figure 1B in Gobler and Sunda 2012), the cell has a layered covering akin to a PT, and judging from the thickness, has four layers. The magnification was too low to see pores, but the overall structure strongly resembles images of *W. julieharrissiae* (Fig. 3a) and *Chromopallida australis* (Fig. 7a) from the Pelagomonadales. The cell covering of *Pelagomonas* has not been studied following HPF fixation, but a thin theca has been described (Andersen et al. 1993). It seems

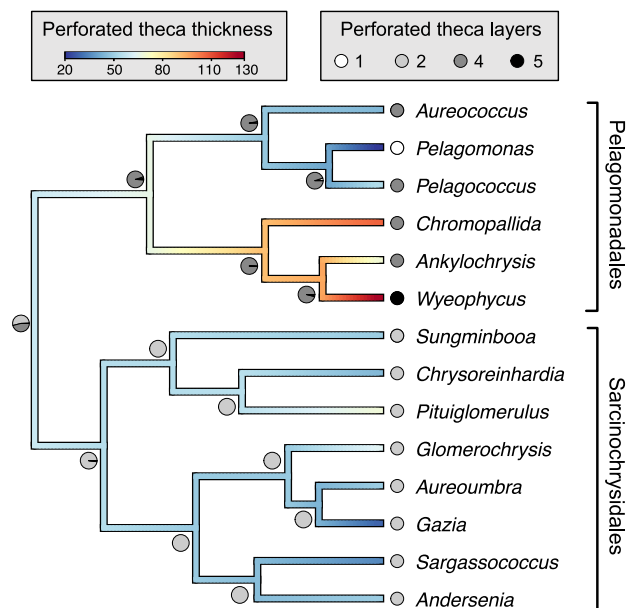


FIG. 13. Chronogram showing inferred ancestral states for the overall thickness and layering of the PT. The color indicated on branches indicates the thickness of the PT and the circles the number of theca layers. The proportions of the circles drawn in different shades of gray indicate the probabilities of corresponding trait states. [Color figure can be viewed at wileyonlinelibrary.com]

TABLE 1. Perforated Theca Data. Data for the 14 pelagophyte genera studied thus far with TEM where information on the PT is available are listed, including the two species of *Gazia* where the PT is different.

Taxon	PT layers	PT thickness	Layer #1	Layer #2	Layer #3	Layer #4	Layer #5	Pore types	Micropore size	Macropore size
Pelagomonadales										
<i>Wyeophycus</i> ^a	5	120–140 nm	25–30 nm	20–30 nm	20–25 nm	20–30 nm	20 nm+	2	10–12 nm	20–25 nm
<i>Chromohalida</i> ^a	4	100–125 nm	20–25 nm	40–50 nm	20–25 nm	20–25 nm	None	1	10–12 nm	18–20 nm
<i>Ankylochrysis</i>	4	65–75 nm	c. 20 nm	c. 25 nm	c. 20 nm	c. 12 nm	None	2	10–12 nm	18–20 nm
<i>Pelagococcus</i>	4	50–60 nm	20–25 nm	15–20 nm	15–20 nm	12–14 nm	None	1	12–14 nm	None
<i>Aureococcus</i>	4?	40–50 nm	?	?	?	?	None	?	?	?
<i>Pelagomonas</i>	1?	?	?	None	None	None	None	?	?	?
Sarcinochrysidales										
<i>Pituiglomerulus</i> ^a	2	Variable	Variable	25–30 nm	None	None	None	1	None	20–22 nm
<i>Chrysoreinhardtia</i> ^a	2	40–50 nm	12–18 nm	25–35 nm	None	None	None	1	10–12 nm	None
<i>Sungminbooa</i> ^a	2	45–55 nm	0–10 nm	45–55 nm	None	None	None	1	12–14 nm	None
<i>Glomerochrysis</i> ^b	2	60–70 nm	20–24 nm	40–45 nm	None	None	None	1	None	18–22 nm
<i>Aureoumbra</i> ^b	2	45–55 nm	12–15 nm	35–45 nm	None	None	None	1	None	18–20 nm
<i>Gazia saundersii</i> ^b	2	25–30 nm	12–15 nm	12–15 nm	None	None	None	1	None	18–22 nm
<i>Gazia australica</i> ^b	2	70–90 nm	10–12 nm	60–80 nm	None	None	None	2	5–8 nm	20–22 nm
<i>Sargassococcus</i> ^a	2	30–40 nm	20–24 nm	12–14 nm	None	None	None	1	None	18–22 nm
<i>Andersenii</i> ^a	2	45–55 nm	20–25 nm	25–30 nm	None	None	None	1	10–12 nm	None

^aGenera where the PT is described in this paper.

^bGenera described in Wetherbee et al. (2021). Other genera listed had results previously published, see discussion.

unlikely that this tiny flagellate has a four or five layered PT, and if true, that would make it the only known exception in the Pelagomonadales.

A bilayered PT is observed in the Sarcinochrysidales where the main differences between genera are in the thickness of layers 1 and 2 and the size of the pores in layer 2 (see summary, Table 1). *Pituiglomerulus capricornicus* is characterized by an undulating PT resulting from a major variation in the thickness of layer 1, a feature that has been only observed in this genus thus far. Layer 2 follows the contour of layer 1 and has tightly packed macropores with a diameter of 20–22 nm, while the thickness of layer 2 is only 25–30 nm (e.g., Fig. 8g). In several genera the PT appears as train tracks, some with obvious track ‘ties’ connecting the PM and layer 2, this feature being particularly obvious in *Glomerochrysis* (Fig. 7g in Wetherbee et al. 2021) and *Sargassococcus* (see Fig. 11a) where layer 2 is only marginally thicker (12–15 nm) than the PM. Layer 2 is thicker (25–35 nm) in *Chrysoreinhardtia* and *Andersenii* and much thicker in *Sungminbooa*, *Glomerochrysis*, *Ga. australica* and *Aureoumbra* (35–80 nm) where layer 2 dominates the PT (Table 1.).

PT pores come in two types, micropores (8–14 nm in diameter) and macropores (18–25 nm; Table 1). Pores are best seen in tangential section, as the sections themselves are typically 70–80 nm thick and the matrix the pores are embedded in is electron dense. Individual micropores can be hard to discern in cross-sections, but overall they give layer 2 the appearance of being porous, or aerated (e.g., *Chrysoreinhardtia*, Fig. 9, l–n). Some genera have either micropores or macropores, while other genera have both (Table 1; also see fig. 6, e and f, in Wetherbee et al. 2021). In conclusion, 14 of the known 20 genera of the Pelagophyceae have been shown by our studies, or from published reports by other researchers, to have a multilayered PT.

Novel features of the endomembrane system and secretion. Not all features reported here can be confirmed for all genera studied, as the quality of the HPF preservation varied for some components of the endomembrane system. As the PT has been shown to encase entire cells except where flagella emerge, there are no regions on the cell surface devoid of the PT with direct access for vesicle secretion into the extracellular space without the involvement of the PT. We have observed two types of vesicle secretion in the pelagophytes. Firstly, standard secretion where vesicles containing PT rafts fuse directly with the PM to insert rafts into an expanding PT. The second mechanism of secretion deploys materials for the formation of the ECM, the cell wall and mucilage layers that self-assemble outside the PT. In this case membrane-bound secretory vesicles are not observed to fuse with the PM, but rather are repositioned intact into the extracellular space within layer 1 of the PT, eventually disintegrating and releasing their contents. This is a novel

strategy for secretion not observed in other algal systems to our knowledge.

The most complete results for PT formation were in *Wyeophycus julieharrissiae*, which showed the secretion of complex, four layered PT rafts fabricated in vesicles of the endomembrane system, presumably originating from the Golgi. The PT raft vesicles possess both contents destined for incorporation into the surface PT plus a surrounding vesicle membrane that recognizes and fuses with the PM, the standard strategy for secretion seen in most eukaryotic cells. The fabrication of large thecal rafts within vesicles of the endomembrane system is unusual, not only in the pelagophytes, but also the heterokonts and algae in general. The multilayered rafts are assembled within multilayered vesicles, developing the 4 layers of the PT in precise order while enclosed within the vesicle membrane. Mature rafts are assembled with an opening to fuse with the PM/PT complex, the rafts inverting during secretion, the inner layer becoming the outer layer 4 in the PT (e.g., Fig. 4, k–m). Layer 5 is not obvious within PT rafts and appears to form and develop following secretion. During intense PT formation (e.g., prior to and during the division cycle), large pockets of cytoplasm are observed within the chloroplast lobes where differentiating PT rafts are obvious (Fig. 4, b–d), even in the light microscope (Fig. 2, f–h). Mature rafts in PT vesicles appear adjacent to the PM as well as images illustrating their secretion and resulting addition into the PM-PT complex. The formation of ornate wall components (e.g., scales, bristles, spines, coccoliths, etc.) either by cis-teral progression within the Golgi stack or within vesicles derived from the Golgi is common in the algae, but the formation and deployment of multilayered coverings in Golgi-derived vesicles is unusual. Layered coverings of the ECM that enclose cells are normally self-assembled from products secreted on the cell surface (see below), and do not arrive at the surface fully formed.

Chromopallida australis has a 4 layered PT much like *Wyeophycus julieharrissiae*, as well as electron dense vesicles apparently derived from the Golgi apparatus (GA) with a perforated content like seen in the PT (Fig. 7f). Multilayered vesicles with electron dense regions the same thickness as the PT often accumulate near the PM (Fig. 7i), but the contents lack the detail observed for *W. julieharrissiae* and these vesicles have not been observed fusing with the PM. Unfortunately, few cells of this species were concentrated in the HPF pellets so many of the developmental stages we observed *W. julieharrissiae* are lacking. Likewise, there are no other published reports from this lineage that describe PT formation.

An ECM including cell walls and mucilage layers that cover the entire surface of cells is common in major groups of the algae, including divisions of the green algae, red and brown algae. Even the most

complex and multilayered ECMs are fabricated extracellularly from precursor molecules synthesized and secreted within Golgi-derived vesicles. Some of these coverings have highly ornamental features such as spines, combs and warty layers (e.g., in the green alga *Scenedesmus*, Staehelin and Pickett-Heaps 1975), all having self-assembled extracellularly. In benthic pelagophytes the PT is typically overlain by an ECM comprised of cell wall and/or mucilage layers that likewise self-assemble.

The second, novel type of vesicle secretion in pelagophytes appears to provide materials for the development of the ECM layers and utilizes a mechanism of secretion that has not been observed in other algae, or other eukaryotes that we are aware of. The processes involved in extracellular vesicle secretion are not understood in detail, but are significantly different from classic secretion where secretory vesicles are surrounded by membrane that has been modified by the Golgi to both recognize and then fuse with the PM, depositing a Golgi-derived product into the extracellular space. This mechanism preserves the continuity of the PM that by necessity always remains intact. In TEM images presented here for pelagophytes, it is hard to discern exactly how the membrane-bound vesicles migrate into the extracellular space while also maintaining the integrity of the PM. All the evidence points to the secretory vesicle membrane not recognizing the PM, thus preventing fusion and requiring an alternative mode of secretion. Blebbing would be a possible answer, but stages of blebbing have not been observed nor have we observed extracellular vesicles surrounded by two membranes that would presumably result from blebbing. What TEM images do show is vesicles with a portion of their membrane tightly appressed to the PM surface (arrows, Fig. 10, f and g), with a fibrous material appearing to adhere them together. In response to a vesicles presence, a new segment of PM then appears to be synthesized on the cytoplasmic side of the vesical as the original segment of PM degrades, the overall result being the expulsion of the entire vesicle into the extracellular space between the PM and PT (see Fig. 10, f–j). The final act of secretion occurs when the extracellular vesicles disintegrate, releasing the vesicle contents (e.g., Fig. 10, k and l). The PT would then mediate the passage of vesicle products to an outer position where wall and/or mucilage layers would assemble.

Peripheral vesicles that are common in many pelagophytes (e.g., Han et al. 2018) are another type of vesicle observed to accumulate in close association with the PM, for example *Sargassococcus* (Fig. 11), and contain lightly stained, nondescript contents. Peripheral vesicles were never observed to either fuse with the PM or to be expelled in their entirety as discussed above. Large enough to see in the light microscope, peripheral vesicles appeared to maintain their size and position near the cell

surface when observed under low light for 2 h or more. We have no evidence that they are ever secreted and it's entirely possible that they are storage vesicles as they appear to accumulate further in cells from older cultures.

In *Wyeophycus julieharrissiae* and *Chromopallida australis* from the Pelagomonadales, cells appeared to have Golgi stacks in two functional states as defined by the accumulated vesicles at their distal, mature faces. Vesicles either had electron dense contents with structural features of the PT that dominated during the division cell cycle, or the Golgi stacks produced smaller vesicles with a different morphology that were more frequently observed. Multilayered vesicles, or vesicles within vesicles, were commonly observed, and images suggested they might arise from the fusing of one type of vesicle with another (e.g., Figs. 4e; 10, c and d), resulting in compartments where the contents appeared different. Other species illustrated here were observed to have many of the same features of endomembrane structure and function, and together they may help define the Pelagophyceae.

The endomembrane system in the formation of complex cell coverings. The production of ornate cell coverings is common in many algal divisions, but typically results from the accumulation of wall components individually secreted onto the surface, not from the formation of several distinct wall layers into rafts. For example, the formation of species-specific organic scales by cisternal progression in the Golgi is common in many prasinophytes (green algae). In some species (e.g., *Tetraselmis*; Becker et al. 1991), scales accumulate on the cell surface and are glued together to form a wall, while in other prasinophytes (e.g., *Pyramimonas*; Moestrup and Walne 1979), scales accumulate within a scale reservoir to form multilayered rafts comprised of several different scale types before being secreted onto the surface at a precise location adjacent to the basal bodies. These scale rafts are totally different from the PT rafts described here, that are formed within a single vesicle and not from an accumulation of several Golgi-derived entities.

Other examples of the formation and secretion of highly ornamental surface units by the endomembrane system include the Golgi-derived organic scales and calcified coccoliths in some haptophytes (e.g., *Pleurochrysis* and *Emiliania*; for reviews see Green 1986, Faber and Preisig 1994). Once again, coccoliths are fabricated and secreted individually, subsequently accumulating on the surface to form a covering, or coccosphere, which may contain two or more types of coccoliths in precise arrays that are species-specific.

In the heterokont class Synurophyceae (e.g., *Mallomonas*) "silica deposition vesicles", which appear to be derived from the GA, manufacture ornate silicified scales and bristles that are prepositioned within the cytoplasm by a microtubule/actin

cytoskeleton prior to secretion into a precise position within an established scale case (Beech et al. 1990, Lavau and Wetherbee 1994). Unlike *Wyeophycus julieharrissiae* where all PT rafts appear structurally identical to the surface PT, scale cases of *Mallomonas* possess an exact number of scales and bristles, each component a specific size and morphology depending on its surface position. Scale cases double in size prior to division, involving the continuous insertion of single scales/bristles of the correct measurements into the established scale cases where they adhere at specific locations (Beech et al. 1990, Lavau and Wetherbee 1994). This is a very different process than PT formation in *W. julieharrissiae* but demonstrates the multifaceted role of the GA and endomembrane system in the fabrication of ornate, species-specific cell coverings in the algae.

CONCLUSIONS

Sarcinochrysis was described about 100 years ago (Geitler 1930), but the class Pelagophyceae was described less than 30 years ago with a single species (Andersen et al. 1993). Currently, including this paper, there are 27 described species and 20 genera. On one hand, all known species inhabit the marine environments, with most species occurring in coastal areas; to our knowledge there are no pelagophyte environmental sequences from freshwater habitats. Morphologically, all species have a layered PT covering the cells that is fabricated in a novel mechanism involving rafts developed in Golgi vesicles. In addition, outer wall and mucilage layers are generated from Golgi-derived, extracellular vesicles that release their contents between the PM and PT, a novel mechanism of secretion in the algae.

Generally speaking, the Pelagomonadales showed much more variation in PT traits than the Sarcinochrysidales. This includes high variability of the overall PT thickness, which is thin in the *Aureococcus-Pelagomonas-Pelagococcus* lineage and thick in the *Chromopallida-Ankylochrysis-Wyeophycus* clade, whereas Sarcinochrysidales feature more intermediate thecal thicknesses (Fig. 13). Similarly, Sarcinochrysidales were uniform in the number of thecal layers whereas Pelagomonadales were not (Fig. 13). Since all pelagophytes have a PT with an apparently novel mode of formation, it stands to reason that the PT evolved in a common ancestor of the class. However, the nature of this PT could not be inferred with confidence. In terms of layering, we obtained similar probabilities for two or four layers for the ancestral PT. There was also substantial uncertainty on the estimate for overall thecal thickness in the pelagophyte most recent common ancestor. While we can project that the PT has a structural role plus protection from invading microbes and micrograzers, the exact function of this unique covering remains unknown.

We greatly appreciate and acknowledge the expert advice on nomenclature by Michael D. Guiry, National University of Ireland, Galway, and valuable comments on the manuscript by David Mann. We thank the School of Biosciences Microscopy Unit at the University of Melbourne for the use of the electron microscopes and accessory equipment, and the RMIT Microscopy and Microanalysis Facility for the use of their high-pressure freezer. Financial support was provided by the Australian Biological Resources Study (Activity ID 4-G046 to HV), the University of Melbourne (McKenzie fellowship to TTB) and the University of Melbourne Botany Foundation. Open access publishing facilitated by The University of Melbourne, as part of the Wiley - The University of Melbourne agreement via the Council of Australian University Librarians.

REFERENCES

- Abascal, F., Zardoya, R. & Telford, M. J. 2010. TranslatorX: multiple alignment of nucleotide sequences guided by amino acid translations. *Nucleic Acids Res.* 38:W7–W13.
- Andersen, R. A., Saunders, G. W., Paskind, M. P. & Sexton, J. P. 1993. Ultrastructure and 18 S rRNA gene sequence for *Pelagomonas calceolata* gen. et sp. nov. and the description of a new algal class, the Pelagophyceae classis nov. *J. Phycol.* 29:701–15.
- Becker, B., Becker, D., Kamerling, J. P. & Melkonian, M. 1991. 2-Keto-sugar acids in green flagellates: a chemical marker for prasinophycean scales. *J. Phycol.* 27:498–504.
- Beech, P. L., Wetherbee, R. & Pickett-Heaps, J. D. 1990. Secretion and deployment of bristles in *Mallomonas splendens* (Synurophyceae). *J. Phycol.* 26:112–22.
- Bricelj, V. M. & Lonsdale, D. J. 1997. *Aureococcus anophagefferens*: causes and ecological consequences of brown tides in U.S. mid-Atlantic coastal waters. *Limnol. Oceanogr.* 42:1023–38.
- Buskey, E. J., Liu, H., Collumb, C. & Bersano, J. G. F. 2001. Decline and recovery of a persistent Texas brown tide algal bloom in the Laguna Madre (Texas, USA). *Estuaries* 24:337–46.
- Cremen, M. C. M., Huisman, J. M., Marcelino, V. R. & Verbruggen, H. 2016. Taxonomic revision of *Halimeda* (Bryopsidales, Chlorophyta) in south-Western Australia. *Aust. Syst. Bot.* 29:41–54.
- Cremen, M. C. M., Leliaert, F., Marcelino, V. R. & Verbruggen, H. 2018. Large diversity of nonstandard genes and dynamic evolution of chloroplast genomes in siphonous green algae (Bryopsidales, Chlorophyta). *Genome Biol. Evol.* 10:1048–61.
- Cremen, M. C. M., Leliaert, F., West, J., Lam, D. W., Shimada, S., Lopez-Bautista, J. M. & Verbruggen, H. 2019. Reassessment of the classification of Bryopsidales (Chlorophyta) based on chloroplast phylogenomic analyses. *Mol. Phylogenet. Evol.* 130:397–405.
- Davison, J. R. & Bewley, C. A. 2019. Antimicrobial chrysophaentin analogs identified from laboratory cultures of the marine microalga *Chrysophaeum taylorii*. *J. Nat. Prod.* 148:148–53.
- Derelle, R., Lopez-Garcia, P., Timpano, H. & Moreira, D. 2016. A phylogenetic framework to study the diversity and evolution of stramenopiles (= Heterokonts). *Mol. Biol. Evol.* 33:2890–8.
- DeYoe, H. R., Stockwell, D. A., Bidigare, R. R., Latasa, M., Johnson, P. W., Hargraves, P. E. & Suttle, C. A. 1997. Description and characterization of the algal species *Aureoumbra lagunensis* gen. et sp. nov. and referral of *Aureoumbra* and *Aureococcus* to the Pelagophyceae. *J. Phycol.* 33:1042–8.
- Dorrell, R. G. & Bowler, C. 2016. Secondary plastids of stramenopiles. In Hirakawa, Y. [Ed.] *Advances in Botanical Research*, Vol. 84. Academic Press, Cambridge, MA, USA, pp. 57–103.
- Dorrell, R. G., Gile, G., McCallum, G., Méheust, R., Baptiste, E. P., Klinger, C. M., Brillet-Guéguen, L., Freeman, K. D., Richter, D. J. & Bowler, C. 2017. Chimeric origins of ochrophytes and haptophytes revealed through an ancient plastid proteome. *Elife* 6:e23717.
- Edgar, R. C. 2004. MUSCLE: multiple sequence alignment with high accuracy and high throughput. *Nucleic Acids Res.* 32:1792–7.
- Faber, W. W. & Preisig, H. R. 1994. Calcified structures and calcification in protists. *Protozoology* 181:78–105.
- Gayral, P. & Billard, C. 1977. Synopsis du nouvel ordre des Sarcinochrysidales (Chrysophyceae). *Taxon* 26:241–5.
- Geitler, L. 1930. Ein grünes Filarplasmidium und andere neue Protisten. *Arch. f. Protistenk.* 69:615–36.
- Gobler, C. J., Berry, D. L., Dyhrman, S. T., Wilhelm, S. W., Salamov, A., Lobanov, A. V., Zhang, Y. et al. 2011. Niche of harmful alga *Aureococcus anophagefferens* revealed through ecogenomics. *Proc. Natl. Acad. Sci. USA* 108:4352–7.
- Gobler, C. J. & Sunda, W. G. 2012. Ecosystem disruptive algal blooms of the brown tide species, *Aureococcus anophagefferens* and *Aureoumbra lagunensis*. *Harmful Algae* 14:36–45.
- Graf, L., Yang, E. C., Han, K. Y., Kupper, F. C., Benes, K. M., Oyamomari, J. K., Herbert, J. H., Verbruggen, H., Wetherbee, R., Andersen, R. A. & Yoon, H. S. 2020. Multigene phylogeny, morphological observation and re-examination of the literature lead to the description of the Phaeosacciphyceae classis nova and four new species of the Heterokontophyta S1 clade. *Protist* 171:1–26.
- Grant, B., Waller, R. F., Clementson, L. & Wetherbee, R. 2013. *Psammomonas australis* gen. et sp. nov. (Raphidophyceae), a new dimorphic, sand-dwelling raphidophyte from southeastern Australia. *Phycologia* 52:57–64.
- Grant, B., Waller, R. F. & Wetherbee, R. 2011. *Platyachrysis moestrupii* sp. nov. (Prymnesiophyceae): a new dimorphic, sand-dwelling haptophyte species from southeastern Australia. *Phycologia* 50:608–15.
- Green, J. C. 1986. Biomineralization in the algal class Prymnesiophyceae. In Leadbeater, B. S. C. & Riding, R. [Eds.] *Biomineralization in lower plants and animals*. Clarendon Press, Oxford, pp. 173–88.
- Han, K. Y., Graf, L., Reyes, C. P., Melkonian, B., Andersen, R. A., Yoon, H. S. & Melkonian, M. 2018. A re-investigation of *Sarcinochrysis marina* (Sarcinochrysidales, Pelagophyceae) from its type locality and the descriptions of *Arachmochrysis*, *Pelagospilus*, *Sargassococcus* and *Sungminbooa* genera nov. *Protist* 169:79–106.
- Hanaichi, T., Sato, T., Hoshin, M. & Mizuno, N. 1986. A stable lead stain by modification of Sato's method. *Proc XIth Int. Cong. On Electron Microscopy, Kyoto*. pp. 2181–2.
- Honda, D. & Inouye, I. 1995. Ultrastructure and reconstruction of the flagellar apparatus architecture in *Ankylochrysis lutea* (Chrysophyceae, Sarcinochrysidales). *Phycologia* 34:215–27.
- Jackson, C., Knoll, A. H., Chan, C. X. & Verbruggen, H. 2018. Plastid phylogenomics with broad taxon sampling further elucidates the distinct evolutionary origins and timing of secondary green plastids. *Sci. Rep.* 8:1523.
- Kearse, M., Moir, R., Wilson, A., Stones-Havas, S., Cheung, M., Sturrock, S., Buxton, S. et al. 2012. Geneious Basic: an integrated and extendable desktop software platform for the organization and analysis of sequence data. *Bioinformatics* 28:1647–9.
- Keller, M. D., Selvin, R. C., Claus, W. & Guillard, R. R. L. 1987. Media for the culture of oceanic ultraphytoplankton. *J. Phycol.* 23:633–8.
- Lavau, S. & Wetherbee, R. 1994. Structure and development of the scale case of *Mallomonas adamas* (Synurophyceae). *Protozoology* 181:259–68.
- Lewin, J., Norris, R. E., Jeffrey, S. W. & Pearson, B. E. 1977. An aberrant chrysophycean alga *Pelagococcus subviridis* gen. et sp. nov. from the North Pacific Ocean. *J. Phycol.* 13:259–66.
- Lobban, C. S., Honda, D., Chihara, M. & Scheffer, M. 1995. *Chrysoecystis fragilis* gen. nov., sp. nov. (Chrysophyceae, Sarcinochrysidales), with notes on other macroscopic chrysophytes (golden algae) on Guam reefs. *Micronesica* 28:91–102.
- Marcelino, V. R., Cremen, M. C. M., Jackson, C. J., Larkum, A. & Verbruggen, H. 2016. Evolutionary dynamics of chloroplast genomes in low light: a case study of the endolithic green alga *Ostreobium quekettii*. *Genome Biol. Evol.* 8:2939–51.

- Moestrup, Ø. 2021. The strange Pelagophyceae: now also defined ultrastructurally? *J. Phycol.* 57:393–5.
- Moestrup, Ø. & Walne, P. L. 1979. Studies on scale morphogenesis in the Golgi apparatus of *Pyramimonas tetrahychnus* (Prasinophyceae). *J. Cell Sci.* 36:437–59.
- Popescu, A. A., Huber, K. T. & Paradis, E. 2012. ape 3.0: New tools for distance-based phylogenetics and evolutionary analysis in R. *Bioinformatics* 28:1536–7.
- Preisig, H. R., Anderson, O. R., Corliss, J. O., Moestrup, Ø., Powell, M. J., Roberson, R. W. & Wetherbee, R. 1994. Terminology and nomenclature of protist cell surface structures. *Protoplasma* 181:1–28.
- R Core Team 2021. *R: A language and environment for statistical computing*. R Foundation for Statistical Computing, Vienna, Austria <https://www.R-project.org/>.
- Revell, L. J. 2012. phytools: An R package for phylogenetic comparative biology (and other things). *Methods Ecol. Evol.* 3:217–23.
- Sanderson, M. J. 2002. Estimating absolute rates of molecular evolution and divergence times: a penalized likelihood approach. *Mol. Biol. Evol.* 19:101–9.
- Saunders, G. W., Potter, D. & Andersen, R. A. 1997. Phylogenetic affinities of the Sarcinochrysidales and Chrysomeridales (Heterokonta) based on analyses of molecular and combined data. *J. Phycol.* 33:310–8.
- Saunders, G. W., Potter, D., Paskind, M. P. & Andersen, R. A. 1995. Cladistic analyses of combined traditional and molecular data sets reveal an algal lineage. *Proc. Natl. Acad. Sci. USA* 92:244–8.
- Sieburth, J. M. N., Johnson, P. W. & Hargraves, P. E. 1988. Ultrastructure and ecology of *Aureococcus anophagefferens* gen. et sp. nov. (Chrysophyceae): the dominant picoplankton during a bloom in Narragansett Bay, Rhode Island, summer 1985. *J. Phycol.* 24:416–25.
- Spurr, A. R. 1969. A low-viscosity epoxy resin embedding medium for electron microscopy. *J. Ultrastruct. Res.* 26:3143.
- Stachelin, L. A. & Pickett-Heaps, J. D. 1975. The ultrastructure of *Scenedesmus* (Chlorophyceae). 1. Species with the “reticulate” or “warty” type of ornamental layer. *J. Phycol.* 11:186–202.
- Stamatakis, A. 2014. RAxML version 8: a tool for phylogenetic analysis and post-analysis of large phylogenies. *Bioinformatics* 30:1312–3.
- van der Veer, J. 1970. *Ankylochrysis lutea* (Chrysophyta), a new species from the Tamar Estuary, Cornwall. *Acta Bot. Neerland* 19:616–36.
- Vesk, M. & Jeffrey, S. W. 1987. Ultrastructure and pigments of two strains of the picoplanktonic alga *Pelagococcus subviridis* (Chrysophyceae). *J. Phycol.* 23:322–36.
- Wetherbee, R., Bringloe, T. T., Costa, J. F., van de Meene, A., Andersen, R. A. & Verbruggen, H. 2021. New pelagophytes show a novel mode of algal colony development and reveal a perforated theca that may define the class. *J. Phycol.* 57:396–411.
- Wetherbee, R., Gornik, S. G., Grant, B. & Waller, R. F. 2015. *Andersenina*, a genus of filamentous, sand-dwelling Pelagophyceae from southeastern Australia. *Phycologia* 54:35–48.
- Wetherbee, R., Jackson, C. J., Repetti, S. I., Clementson, L. A., Costa, J. F., van de Meene, A., Crawford, S. & Verbruggen, H. 2019b. The golden paradox – a new heterokont lineage with chloroplasts surrounded by two membranes. *J. Phycol.* 55:257–78.
- Wetherbee, R., Marcelino, V. R., Costa, J. F., Grant, B., Crawford, S., Waller, R. F., Andersen, R. A., Berry, D., McFadden, G. I. & Verbruggen, H. 2019a. A new marine prasinophyte genus alternates between a flagellate and a dominant benthic stage with microrhizoids for adhesion. *J. Phycol.* 55:2010–25.
- Wetherbee, R. & Verbruggen, H. 2016. *Kraftionema allantoideum*, a new genus and family of Ulotrichales (Chlorophyta) adapted for survival in high intertidal pools. *J. Phycol.* 52:701–15.
- Wynne, M. J., Andersen, R. A., Graf, L. & Yoon, H. S. 2014. *Aureoscheda*, a new genus of marine Pelagophyceae from The Bahamas, Caribbean Sea. *Phycologia* 53:513–22.
- Yang, E. C., Boo, G. H., Kim, H. J., Cho, S. M., Boo, S. M., Andersen, R. A. & Yoon, H. S. 2012. Supermatrix data highlight the phylogenetic relationships of photosynthetic stramenopiles. *Protist* 163:217–31.

Supporting Information

Additional Supporting Information may be found in the online version of this article at the publisher's web site:

Figure S1. Phylogenetic tree of the Pelagophyceae inferred from the 18S rDNA gene. This tree includes additional taxa compared to Figure 1, mostly species for which only the 18S rDNA gene is available. The three newly described taxa are indicated with a star, and sequences not included in Figure 1 with an arrowhead.

Table S1. GenBank accession information for sequences used in phylogenetic analyses, including new accession information for *Wyeophycus julieharrissiae*, *Chromopallida australis*, and *Pituitiglomerulus capricornicus*.